# 4

# RESULTS AND DISCUSSION

The results of the present study entitled "**Validating the potential of *Plectranthus amboinicus* against lung cancer - *In silico, in vitro* and *in vivo* approaches"** are discussed under the following phases.

**PHASE I**

**4.1 PHYTOCHEMICAL SCREENING OF *P. amboinicus* LEAF EXTRACTS**

**PHASE II**

**4.2 FREE RADICAL SCAVENGING ACTIVITY IN THE METHANOLIC EXTRACT OF *P. amboinicus* LEAVES**

4.2.1Determination of DPPH radical scavenging activity

4.2.2 Determination of ABTS radical scavenging activity

4.2.3 Determination of hydrogen peroxide scavenging activity

4.2.4 Determination of inhibition of super oxide radical generation

4.2.5 Determination of inhibition of nitric oxide radical generation

**PHASE III**

**4.3 *IN SILICO* DOCKING OF PHYTOCOMPOUNDS FROM *P. amboinicus* WITH APOPTOTIC TARGETS**

4.3.1 GC-MS analysis in *P. amboinicus* leaf extract

4.3.2 Drug likeness and pharmacokinetic properties

4.3.3 Receptors preparation and molecular docking

4.3.4 Density Functional Theory analysis

4.3.5 Bioactivity score prediction

**PHASE IV**

**4.4 IDENTFICATION OF BIOACTIVE PRINCIPLES IN *P. amboinicus* LEAF EXTRACT**

4.4.1 FT- IR analysis in the methanolic extract of *P. amboinicus*

4.4.2 NMR analysis in the methanolic extract of *P. amboinicus*

4.4.3 Syringic acid fraction extraction by bioassay guided fractionation

4.4.4 UV-Vis spectral analysis of the syringic acid fraction

4.4.5 HPLC analysis of the syringic acid fraction

4.4.6 HPTLC analysis of the syringic acid fraction

**PHASE V**

**4.5 CYTOTOXIC ACTIVITY OF SYRINGIC ACID FRACTION AGAINST A549 HUMAN LUNG CANCER CELLS - AN *IN VITRO* APPROACH**

4.5.1 Cytotoxic activity of A549 cells by MTT dye reduction assay

4.5.2 Nuclear change analyses by AO/EtBr, DAPI and PI staining

4.5.3 Detection of apoptotic events in A549 cells

4.5.4 Determination of cell cycle analysis by Annexin V/FITC staining

4.5.5 Regulation of protein and gene expression by Western Blotting and RT - PCR

4.5.6 Mechanism of SAF in the activation of apoptosis

**PHASE VI**

**4.6 ANTICANCER ACTIVITY OF SYRINGIC ACID FRACTION IN BENZO(A)PYRENE INDUCED EXPERIMENTAL MICE – AN IN VIVO APPROACH**

4.6.1 Acute toxicity study

4.6.2 Effect of syringic acid fraction on tumor growth factors

4.6.2.1 Mean survival time

4.6.2.2 Increased life span

4.6.2.3 Analysis of body weight

4.6.2.4 Analysis of relative lung weight

4.6.3 Effect of syringic acid fraction on hematological parameters

4.6.4 Effect of syringic acid fraction on liver marker enzymes

4.6.5 Effect of syringic acid fraction on renal markers

4.6.6 Effect of syringic acid fraction on tumour marker enzymes

4.6.7 Histopathological studies of the lung tissues

## PHASE I

### 4.1 PHYTOCHEMICAL SCREENING OF P*. amboinicus* LEAF EXTRACTS

Plant extracts and their constituents are regarded as natural products that afford boundless prospect for novel drug discovery due to their immense accessibility and chemical diversity, used in the management of both chronic and deleterious diseases. The anticancer activity of numerous phytochemicals derived from plants was investigated due to its meager adverse reactions. Exploitation of a bioactive principle from plant diversity confide on its extraction, pharmacological screening, isolation and characterization. Hence it is indispensable to find out the presence of phytochemical constituents in plants to ensure their consistency in pharmacological and clinical research. This would facilitate to comprehend the bioactivities and probable adverse effects of active principles which would augment the product quality control (Liang *et al*., 2011).

Extraction is the prime step in the investigation of a plant, as a solvent is involved in the elicitation of the preferred phytoconstituents from the plant resources (Sasidharan *et al*., 2011). The extraction yield of phytocompounds from the plant parts is highly influenced by the extraction methods, extraction time, temperature, pH, solvent, and solvent polarity. Among the solvents used, the methanol extract yielded 54.2%, followed by aqueous extract (43.7%) and petroleum ether extract (38.6%). From the results mentioned above, it can be inferred that methanol extract can elute both the polar and nonpolar phytocompounds resulting in a good extraction yield. Also, it has a good penetration capacity into the cells, thereby extracts both the primary and secondary metabolites. The high yield capacity of *Plectranthus amboinicus* in methanol extract is consistent with similar study conducted by Swamy *et al.* (2017).

Phytochemicals present in plant are excellent bioactive compounds that are being investigated for several therapeutic applications like antimicrobials, anticarcinogens, wound healing, anti-inflammatory, antioxidants and much more. Phytochemicals employed in cancer research exhibit a wide array of mechanism of action against the target cell lines. In line with this, all the detected

phytochemicals in the study are believed to be the pillars in the mechanism of anticancer activity.

The phytochemical screening of the leaf extracts of *P.amboinicus* revealed the presence of various phytochemicals as depicted in Table 3. Methanol extract exhibited the presence of phytochemicals namely, carbohydrates, proteins and amino acids, saponins, alkaloids, phenols, flavonoids, glycosides and sterols, whereas tannins, terpenoids, quinones, anthocyanin, and leucoanthocyanin were found to be absent. As in line with Thaniarasu *et al*. (2015) the leaf extract of *Plectranthus bournea* possessed the phytochemicals such as sterols, flavonoids, reducing sugars, tannins, alkaloids, saponins, amino acids and phenolic compounds which supported our study. Panda *et al.* (2011) observed the presence of phytochemicals such as alkaloids, flavonoids, carbohydrates, glycosides, protein and amino acids, saponins and triterpenoids in the polar extracts (ethanol, methanol and aqueous) of *Cassia fis*tula leaf extracts as compared with nonpolar extracts (petroleum ether and chloroform). Gowdhami *et al*. (2014) acknowledged the existence of bioactive principles in the aqueous and methanol extract of leaves and seeds of *Annona squamosa* as compared with that of the petroleum ether, chloroform and hexane extracts. The results of the present study coincides with Karpe and Lawande (2014) and Sirdaarta *et al*. (2015) who reported the presence of saponins, glycosides, terpenoids, alkaloids, carbohydrates, flavonoids, phenols and tannins in the *Moullava spicata* and in the methanolic extract of *Tasmannia stipitata.*

Table 3 Preliminary phytochemical screening of *Plectranthus amboinicus* leaf extracts

| S. No. | Phytochemicals | Petroleum Ether Extract | Methanol Extract | Aqueous Extract |
|---|---|---|---|---|
| 1 | CARBOHYDRATES | | | |
| | Molisch test | - | +++ | - |
| | Benedict's test | - | +++ | - |
| 2 | PROTEINS AND AMINOACIDS | | | |
| | Ninhydrin test | - | +++ | - |
| | Biuret test | - | +++ | - |
| 3 | SAPONINS | | | |
| | Froth test | - | ++ | - |
| 4 | ALKALOIDS | | | |
| | Mayer's test | - | +++ | + |
| | Dragendroff's test | - | +++ | + |
| | Wagner's test | - | +++ | + |
| 5 | TANNINS | | | |
| | Braemer's test | - | - | - |
| 6 | PHENOLS | | | |
| | Ferric chloride test | + | +++ | + |
| | Lead acetate test | + | +++ | + |
| 7 | FLAVONOIDS | | | |
| | Aqueous NaOH test | + | +++ | + |
| | Schinodo's test | + | +++ | + |
| 8 | GLYCOSIDES | | | |
| | Legal's test | - | ++ | - |
| | Keller's-Killiani test | - | ++ | - |
| 9 | TERPENOIDS | | | |
| | Salkowski test | + | - | + |
| 10 | STEROLS | | | |
| | Libermann – Burchard test | + | ++ | + |
| 11 | QUINONES/ ANTHROQUINONES | | | |
| | Borntrager's test | - | - | - |
| 12 | ANTHOCYANIN | - | - | - |
| 13 | LEUCOANTHOCYANIN | - | - | - |

The composition of bioactive compounds in the plants is considerably influenced by the factors like geographical and ecological features, climatic conditions, and the stage at which the plant material is harvested (Swamy and Sinniah, 2015). According to the published data, *P. amboinicus* roughly contains 76 volatile and 30 non-volatile substances belonging to various phytochemical groups (Arumugam *et al*., 2016). However, in the study, the aqueous extract of *P.amboinicus* reported the presence of alkaloids, phenols, flavonoids, terpenoids and sterols, whereas only phenols, flavonoids, and terpenoids were found in the petroleum ether extract. All the other tested phytochemicals showed no sign of presence in the aqueous and the petroleum ether extracts.

Phenols are the commonly occurring plant compounds that have been researched widely for their anticancer potential against different types of tumors. It has been reported that phenolic compounds can inhibit the activities of oncogenic signaling cascades, angiogenic factors, cyclin-dependent kinases, extracellular signal-regulated kinase (Erk)1/2, and D-type cyclins, which induce uncontrolled proliferation of tumor cells. They are also known to induce apoptosis, prevent cellular migration and metastasis. The herbal extracts abundant in phenolic compounds modulate the intensity of reactive oxygen species in cells thus normalize cell proliferation, survival and apoptosis (Rosa *et al.*, 2016 and Srinivasulu *et al.*, 2018).

Flavonoids are considered as natural chemopreventive substances since they are being explored for the treatment and prevention of cancer widely. They work as an Receptor Tyrosine Kinase inhibitor by impeding the major signal transduction pathways like cell cycle, proliferation, cell migration, and invasion, implicated in lung cancer (Zanoaga *et al.*, 2019). Apigenin which belongs to the class flavones, is evidenced for downregulating the P13k/Akt signaling pathway in human lung cancer cell line (A549), resulting in antiproliferative, antiinvasion, and antimigration effects *(*Zhou *et al.*, 2017). Similarly, flavonoids namely kaempferol, fisetin, hesperetin, naringenin, genistein, and delphinidin are shown to inhibit cell proliferation, cell cycle progression, arrest the G2/M phase, and induce apoptosis and angiogenesis in A549 human lung cancer cell lines (Jin *et al*., 2011;

Kim *et al*., 2017; Ramteke *et al*., 2019; Sonoki *et al*., 2017; Wang and Huang, 2018; Xia *et al.*, 2018; Zhang *et al.*, 2018).

Alkaloids derived from plants have already been commercialized due to their remarkable anticancer properties. To name some, paclitaxel, derived from the bark of *Taxus brivifolia* (Wani *et al*., 1971), camptothecin, discovered from the leaves of *Camptotheca accuminata* (Cragg and Newman, 2005), ellipticine, derived from different parts of *Ochrosia elliptica* (Goodwin *et al.,* 2002), and many more. A recent study with the alkaloid extract of *Moringa oliefera* against the lung cancer cell line by Xie *et al*. (2021) found that they upregulated the expression of caspase 3, caspase 9, and protein p21 while simultaneously downregulated the expression of proteins cyclin D1 and cyclin E, causing cell cycle arrest in A549 cells.

Plant saponins have a wide range of health benefits, including antimicrobial, anti-inflammatory, anti-carcinogenic, immune modulating, and cholesterol lowering properties. The functional metabolism of saponin in cancer treatment involves different molecular mechanisms. Protein is an essential dietary supplement for cancer patients since it aids in the transportation of medications throughout the body, promotes cell development and repair, and improves the immune system. Plant-derived non-digestible carbohydrates are believed to reduce the risk of cancer.

Cardiac glycoside such as acovenoside A when used against A549 non-small-cell lung cancer cells showed selective toxicity to the tumor cell, leaving lung fibroblasts and peripheral blood mononuclear cells intact. In addition, acovenoside A was found to cause apoptosis and DNA damage in A549 cells by disrupting mitochondrial integrity and producing reactive oxygen species (El Gaafary *et al.*, 2017).

Phytosterols play a significant role in cancer treatment and prevention. Several studies have shown that including phytosterols in the diet reduces cancer risk by 20%. Sterols, like other phytochemicals, act against cancer cells by altering membrane composition, integrity, and membrane-bound enzymes, as well

as induce apoptosis, cell cycle arrest, and cytotoxicity (Bradford and Awad, 2007; Normén *et al*., 2001; Suttiarporn *et al*., 2015; Trautwein and Demonty, 2007).

Thus the results of our study reveal the existence of the phytochemicals in methanolic extract of *P. amboinicus* leaves which impart enhanced activity when compared to the petroleum ether and aqueous extracts and hence can be probed for exploiting in the treatment of cancer. Therefore, free radical scavenging activity is carried out using the methanolic extract of *P. amboinicus* was carried out in phase II.

## PHASE II

## 4.2 FREE RADICAL SCAVENGING ACTIVITY IN THE METHANOLIC EXTRACT OF *P. amboinicus* LEAVES

The Phase II of the present study was structured to evaluate the free radical scavenging activity of the methanol extract of *Plectranthus amboinicus* leaves using DPPH, ABTS and hydrogen peroxide scavenging assays, inhibition of superoxide and nitric oxide generation assays.

### 4.2.1 Determination of DPPH radical scavenging activity

DPPH radical scavenging assay is the generally used method to measure the antioxidant activity. DPPH is free stable nitrogen centered radical which accepts an electron or hydrogen radical from an antioxidant to maintain stable diamagnetic molecule (Soare *et al*., 1997). Antioxidants with DPPH radical scavenging activity could contribute hydrogen to free radicals, predominantly to the lipid peroxides or hydroperoxide radicals that are the foremost propagators of the chain autoxidation of lipids, and form non-radical species, resulting in the inhibition of proliferating stage of lipid peroxidation (Bamforth *et al*., 1993).

The antioxidant agent can quench the free radicals thereby results in the decrease of the absorbance at 515 nm. The methanol extract was shown to effectively reduce the stable purple coloured DPPH radical to pale yellow coloured 1, 1 – diphenyl-2-picrylhydrazine (Carmona-Jiménez *et al*., 2014). The free radicals scavenging activity of methanolic extract of *Plectranthus amboinicus* was assessed based on their capability to quench DPPH radical and the results are

depicted in Fig 8. The per cent inhibition was found to be maximum at 100µg/ml, indicating that the leaf extract has the ability to scavenge the free radicals in a concentration dependent manner. The results specify that the radical scavenging activity emerge to be dependent on the presence of phenolics in the leaf extract of *Plectranthus amboinicus*.

The ethanolic extract of *Plectranthus amboinicus* was able to scavenge DPPH and $H_2O_2$ radicals effectively compared to ascorbic acid, the standard. The antioxidant potential might be attributed by the flavonoids and phenols present in *Plectranthus amboinicus* leaf extract (Rai *et al*., 2016).

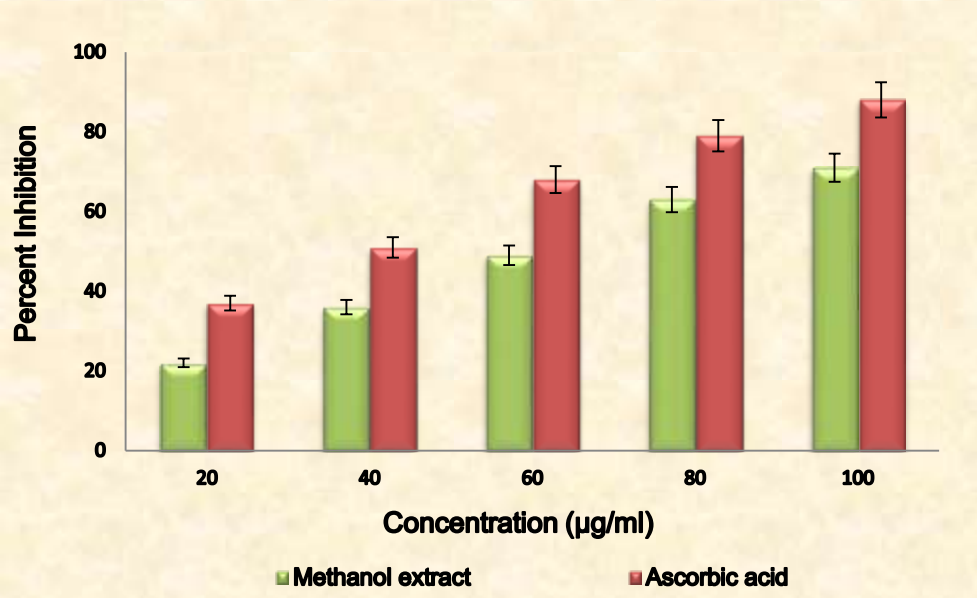


Fig. 8 DPPH radical scavenging activity of methanolic extract of *P. amboinicus*

Phenolics consist of one or more aromatic rings with single or multiple hydroxyl groups and are able to potentially quench the free radicals by forming resonance/stabilized phenoxyl radical (Rabeta and An Nabil, 2013 and Rice-Evans *et al*., 1996). Increasing scavenging activity towards DPPH radicals in methanolic leaf extract was reported in *Vitex negundo* (Bors *et al*., 2002), *Amaranthus spinosus* (Barku *et al*., 2013) and *Phyllanthus amarus, Phyllanthus maderaspatensis, Senna auriculata* and *Solanum torvum* (Ashokkumar *et al*., 2013). Thus the methanolic extract of *Plectranthus amboinicus* revealed strong DPPH scavenging activity comparable with the standard ascorbic acid.

### 4.2.2 Determination of ABTS radical scavenging activity

ABTS radical cation scavenging activity replicates the hydrogen-donating ability. High molecular weight phenolics present in the leaf extracts have high capability to quench free radicals ($ABTS^{\bullet+}$), thus preventing lipid oxidation through chain breaking reaction. It might serve as impending nutraceuticals when ingested along with nutrients (Hagerman *et al*., 1998). The scavenging activity for ABTS radical by methanolic extract of *Plectranthus amboinicus* increased with an increase in concentration (20-100µg/ml) in a dose dependent manner. The highest percent of radical scavenging activity by the methanolic extract of *Plectranthus amboinicus* was observed at 100µg/ml concentration as compared to the standard ascorbic acid (Fig. 9).

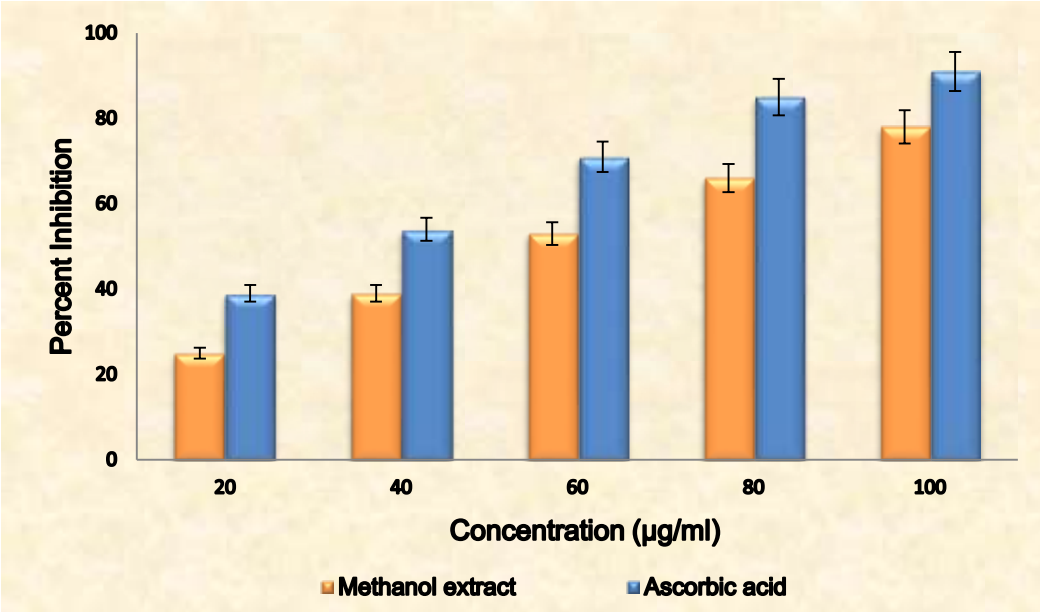


Fig. 9 ABTS radical scavenging activity of methanolic extract of *P. amboinicus*

The methanol extract of *Hippophae rhamnoides* leaves revealed the highest percent inhibition when assessed by ABTS activity (Gill *et al*., 2012). Similar such potent antioxidant and concentration-dependent ABTS radical scavenging activity was observed in the methanolic extract of leaves of *Terminalia catappa* and *Colocasia esculenta* (Chanda *et al*., 2013), *Premna sertatifolia* (Selvam *et al*., 2012), *Coscinum fenestratum* (Goveas *et al*., 2013) and *Salicornia brachiata* (Daffodil *et al*., 2013). The present study revealed that the leaf extract

of *P. amboinicus* was a potent scavenger of ABTS radical as comparable with ascorbic acid, which might be due to the transfer of electrons between the antioxidant and the ABTS radical.

### 4.2.3 Determination of hydrogen peroxide scavenging activity

In the absence of metal ions, hydrogen peroxide ($H_2O_2$) which is a non-radical oxygen species and weak oxidizing agent is stable under biological pH and temperature. It can inactivate few enzymes by the oxidation of thiol groups and shows limited toxicity in a transition-metal free system. The $H_2O_2$ scavenging activity of the leaves extract of *Plectranthus amboinicus* increases with increase in concentration and maximum inhibition was observed at 100ug/ml which is comparable to the scavenging activity of ascorbic acid represented in Fig 10.

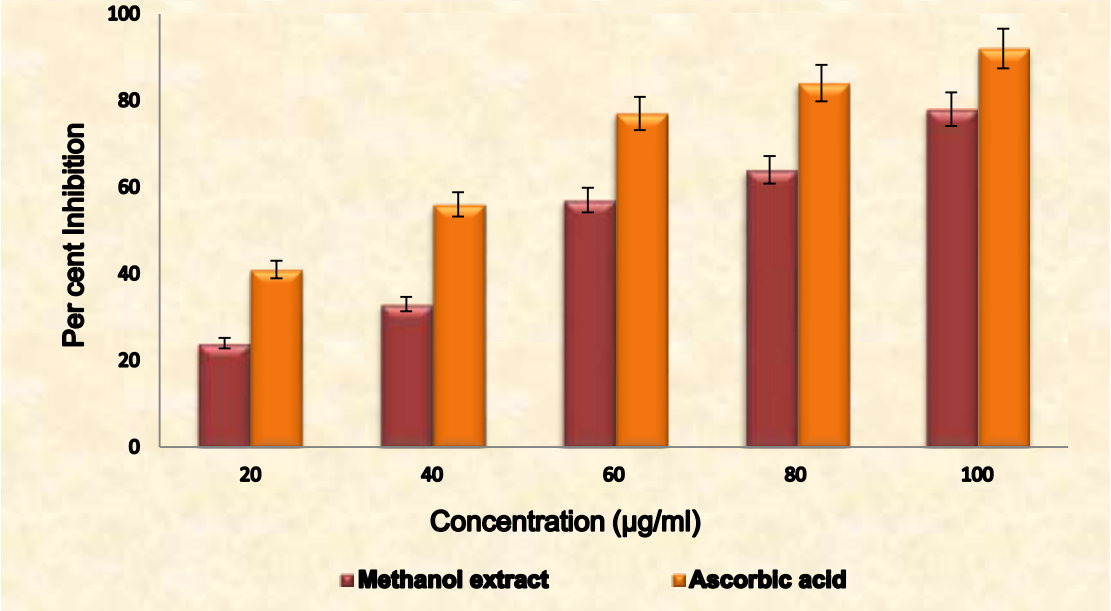


Fig. 10 $H_2O_2$ radical scavenging activity of methanolic extract of *P. amboinicus*

$H_2O_2$ is extremely diffusible and can cross the cell membranes rapidly and react with superoxide anions and metal ions to form hydroxyl radicals, thereby acting as a powerful oxidizing agent, for the cell to control the amount of $H_2O_2$ that is allowed to accumulate (Umamaheswari *et al*., 2015 and Saha *et al*., 2016). $H_2O_2$ itself is not reactive and can be lethal to cells in certain conditions. Hence, its removal is vital for the safety of food systems. The results suggested that the phenolics present in the *Plectranthus amboinicus* may donate electrons to $H_2O_2$

and were able to neutralize it to water to a significant extent by confirming its antioxidant property.

### 4.2.4 Determination of inhibition of super oxide radical generation

The chemical conversion of xanthine to uric acid and electro leakage induced by the activated phagocytes during the mitochondrial electron transport chain leads to the production of superoxide anion ($O_2^{\cdot-}$), an oxygen-centered radical with selective reactivity (Bast *et al*., 1991). Decomposition of superoxide leads to the formation of strong oxidative species namely the hydroxyl radicals and singlet oxygen which may cause damage to the cellular components in a biological system (Ohkawa *et al*., 1979). The superoxide anion radical scavenging activity of methanolic extract of *Plectranthus amboinicus* leaves increased significantly with an increase in concentration, i.e. in a dose-dependent manner. The maximum scavenging activity of superoxide anion was recorded at 100µg/ml, which might be due to the polar nature and the presence of phenolics and antioxidants in the methanolic extract of *Plectranthus amboinicus*. The leaf extract showed equivalent activity with ascorbic acid and the extent of inhibition of superoxide radicals by leaf extract was analysed and presented in Fig 11.

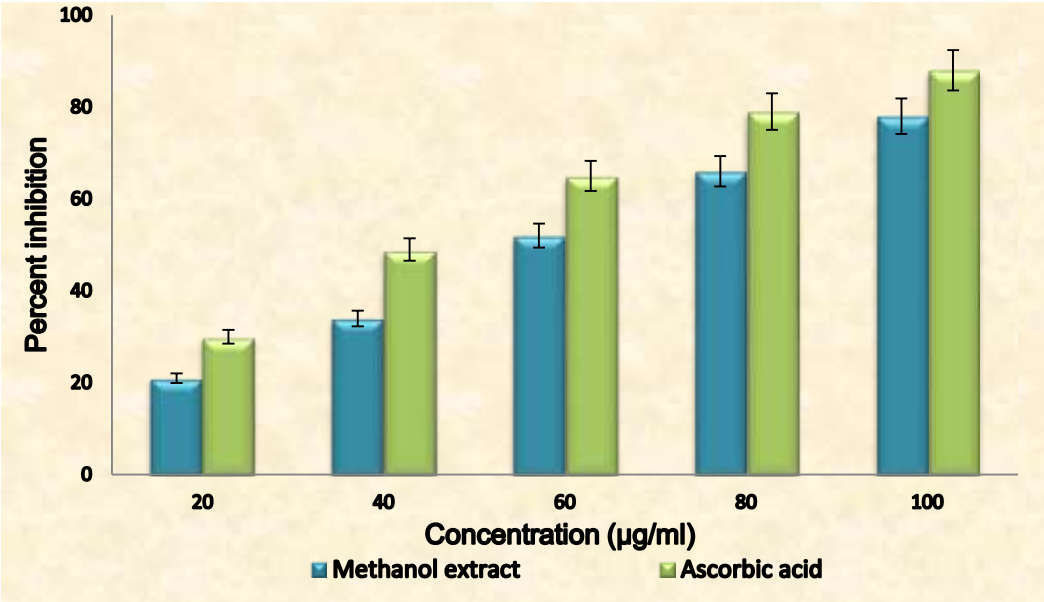


Fig. 11 Inhibition of superoxide radical generation by methanolic extract of *P. amboinicus*

The flavonoids and polyphenols are potent scavengers of hydrogen peroxide, hydroxyl and superoxide radicals and are linked with antioxidant action in biological systems (Jyothi *et al*., 2012). They possess redox activity which plays a critical function in engrossing and deactivating the free radicals, decomposing peroxide and quenching triplet or singlet oxygen (Sarkar *et al*., 2014). The presence of polyphenols in the plant extracts act as effectual hydrogen and electron donors and thus stops the radical chain reaction by transforming free radicals to more stable products (Arya *et al*., 2011). Maximum inhibitory potential of superoxide radical generation by the methanol extract in a dose dependent manner was observed in the stem, bark and leaves of *Cassia fistula* (Siddhuraju *et al*., 2002 and Kumar *et al*., 2008) and *C. alata*, *C. auriculata*, *C. fistula* and *C. simea* (Sujatha *et al*., 2013).

### 4.2.5 Determination of inhibition of nitric oxide radical generation

Nitric oxide acts as a free radical electrophile and also as an oxidising agent. When it combines with oxygen it forms nitrogen dioxide which damages the membrane by quenching hydrogen from unsaturated fatty acids, thereby resulting in auto oxidation (Steinert *et al*., 2010). According to the concept, sodium nitroprusside generates nitric oxide spontaneously in an aqueous solution at physiological pH and interacts with oxygen to produce nitrite ions (Sangameswaran *et al*., 2009). The nitric acid scavengers decreased the oxygen level and the reduced production of nitric ions was monitored at 540nm. The methanolic extract of *Plectranthus amboinicus* can scavenge nitric oxide and hinder the formation of nitrite produced by sodium nitroprusside under *in vitro* conditions. The scavenging activity by the methanolic extract of *Plectranthus amboinicus* exhibited the highest percent of inhibition at 100ug/ml. Both the leaf extract and ascorbic acid inhibited the nitric oxide generation in concentration-dependent manner, as depicted in Fig 12.

Nitric acid is a pro-inflammatory mediator and a diffusible free radical. It is crucial to defend the body and involved in diverse physiological events such as relaxation of smooth muscle, signaling of neurons, regulation of cell-mediated toxicity and inhibition of platelet aggregation (Sirappuselvi and Chitra, 2012).

Excess production of nitric oxide causes tissue damage and activation of pro-inflammatory mediators associated with acute and chronic inflammation (Njoya *et al*., 2017).

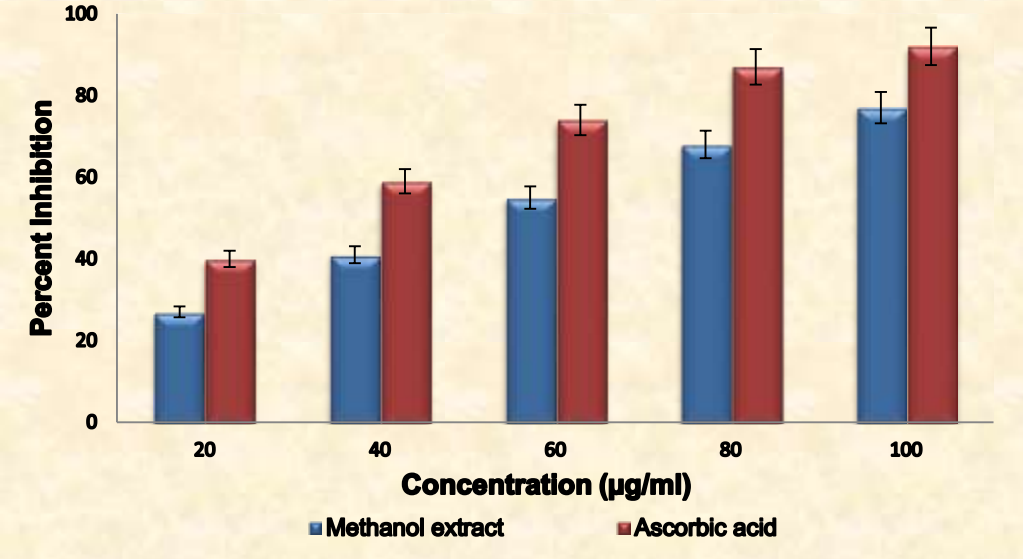


Fig. 12 Inhibition of nitric oxide radical generation by methanolic extract of *P. amboinicus*

A study on the inhibition of nitric oxide generation revealed the highest scavenging activity in the ethanolic extract of *Parinari curatellifolia* leaves followed by *Combretum jeyaheri* and *C. platypetalum* (Boora *et al*., 2014). In agreement with this, the presence of phenolics in the *P. amboinicus* contends with oxygen to react with nitric oxide and thereby inhibiting nitrite formation. The results evidently indicates that the methanolic leaf extract of *Plectranthus amboinicus* exhibited strong scavenging activity towards nitric oxide radical proving its antioxdant potential by inhibiting nitrite ions generations.

The results of phase II revealed that the methanolic extract of *Plectranthus amboinicus* leaves exhibited a promising free radical scavenging effect and thereby prove to be a potent radical scavenger. Further studies necessitate to identify the presence of phytocompounds in the leaf extract of *P. amboinicus* and to evidence them as anticancer agent through *in silico* approach.

## PHASE III

### 4.3 *IN SILICO* DOCKING OF PHYTOCOMPOUNDS FROM *P. amboinicus* WITH APOPTOTIC TARGETS

Docking simulations can be used to study molecular interactions of phytocompounds (ligands) with the target proteins which provide mechanistic insight into the drug development to prevent the growth of various disease causing organisms (Vishwakarma *et al*., 2012). In the study the phytocompounds identified from *Plectranathus amboinicus* was subjected to *in silico* studies to probe their efficacy against apoptotic cancer targets.

#### 4.3.1 GC-MS analysis in *P. amboinicus* leaf extract

The gas chromatogram of *Plectranthus amboinicus* leaf extract depicted the presence of distinctive compounds which were clearly depicted as peaks (Fig. 14) and their retention time, molecular weight, area (%) and structure are tabulated in Table 4.

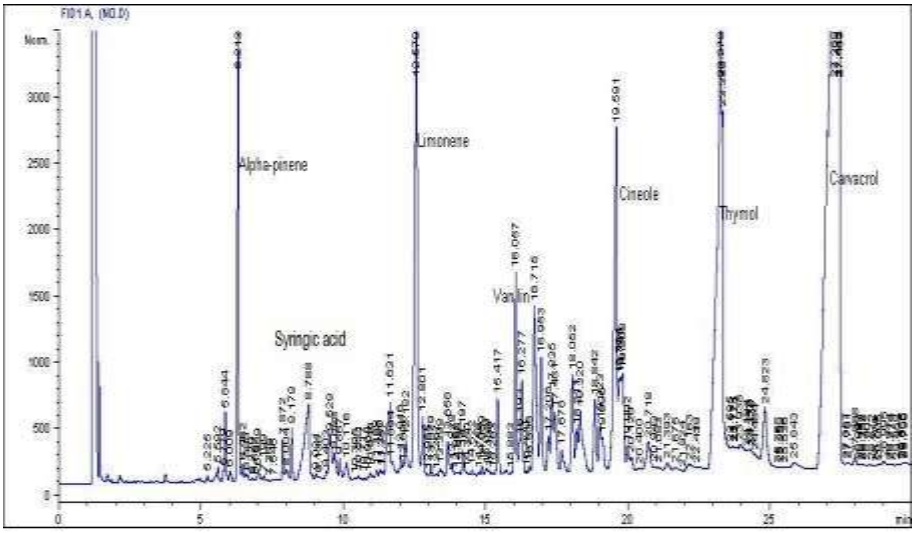


Fig. 13 GC-MS chromatogram of *P. amboinicus* leaf extract

Accordingly, the bioactive compounds such as carvacrol, thymol, alpha pinene, limonene, vanilin, cineole and syringic acid were indicated as seven prominent peaks with the retention time of 27.26, 22.27, 6.31, 12.57, 16.05, 19.59 and 8.76 respectively. The results of the study revealed the presence of compounds with area percentage of 32.66% for carvacrol, 13.02% for thymol,

3.65% for alpha pinene, 6.26% for limonene, 1.75% for vanillin, 4.83% for cineole and 3.22% for syringic acid respectively.

Table 4. Phytocompounds in the leaf extract of *P. amboinicus* analyzed by GC-MS

| S.No | RT | Name of the compound | Molecular weight (g/mol) | Formula | Area (%) | Structure |
|---|---|---|---|---|---|---|
| 1 | 27.26 | Carvacrol | 150.22 | $C_{10}H_{14}O$ | 32.66 | 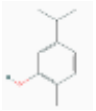 |
| 2 | 19.59 | Cineole | 154.25 | $C_{10}H_{18}O$ | 4.83 |  |
| 3 | 12.57 | Limonene | 136.23 | $C_{10}H_{16}$ | 6.26 | 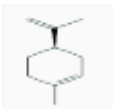 |
| 4 | 6.31 | Pinene | 136.23 | $C_{10}H_{16}$ | 3.65 |  |
| 5 | 8.76 | Syringic Acid | 198.17 | $C_9H_{10}O_5$ | 3.22 | 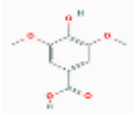 |
| 6. | 23.27 | Thymol | 150.22 | $C_{10}H_{14}O$ | 13.02 | 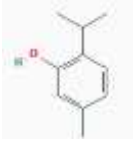 |
| 7. | 16.05 | Vanillin | 152.15 | $C_8H_8O_3$ | 1.75 | 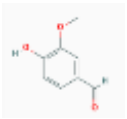 |

While the GC-MS analysis of the essential oil of *Plectranthus amboinicus* contained phytocompounds which included carvocrol - 14%, thymol – 18%, cis – caryophyllene, t-caryophyllen and p-cymene -10% (Manjamalai *et al*., 2012). The results of the GC-MS analysis are consistent with the findings of Barhoi *et al*. (2021) who observed the presence of phenolics, hydrocarbons, fatty acids and quinic acid, 9,12,15-octadecatrienoic acid, hexadecanoic acid, α-tocopherol and γ-sitosterol as bioactive constituents in *Moringa olifera* leaves.

### 4.3.2 Drug likeness and pharmacokinetic properties

The drug-likeness assesses the molecules experimentally based on the physico-chemical and structural properties in order to find out the oral drug candidates with regard to bioavailability. SWISS ADME online tool is used to analyze the pharmacological and pharmacognostic profile of the selected phytocompounds based on five disparate rule based filters namely Lipinski, Ghose, Verber, Egan and Mugge. Drug likeness was assessed to ensure whether the phytocompounds acquire ADME and water soluble properties (Daina *et al*., 2017). Lipinski's rule of five is employed as a tool for accessing the drug-likeness of active compounds and to evaluate whether the compounds are orally active or not. The Lipinski filter (Pfizer) characterize the small molecules based on the physico-chemical properties which includes molecular weight < 500 Da, MLOGP ≤ 5, number of rotatable bonds less than 10 and number of hydrogen bond acceptors and donors less than 10 and 5 respectively (Lipinski *et al*., 2001). Ghose filter (Amgen) describes the physicochemical property, existence of substructures and functional groups of small molecules. The qualifying range comprise the molar refractivity between 40-130, molecular weight between 160 - 480 Da, WlogP between -0.4 to +5.6 and total number of atoms between 20-70 respectively for small molecule (Ghose *et al*., 1999). Veber filter (GSK filter) represents the drug likeness if TPSA (Total Polar Surface Area) is equal to or less than 140 Å with 12 hydrogen bond donors and acceptors and the rotatable bond count should be ≤10. Compounds with these properties will have good oral bioavailability, increased rotatable bond counts has a negative effect on the permeation rate and reduced TPSA correlates with increased permeation rate (Veber *et al*., 2002). The Egan computational model for human intestinal absorption (HIA) of small molecule accounts for active transport and efflux mechanism which predicts whether drug absorption is strong or weak. Egan rule is based on the TPSA and WLogP values which are less than and equal to 131.6 and 5.88 respectively (Egan *et al*., 2000). Muegge filter (Bayer filter) is a self-reliant pharmacophore point filter that segregates drug like and non-drug like molecules. These model symbolizes molecule as a drug like if they have

molecular weight between 200 to 600 Da, XLOGP between -2 and +5, TPSA ≤ 150, Number of rings ≤ 7, Number of carbon atoms > 4, number of heteroatoms > 1, number of rotatable bonds ≤ 15, hydrogen bond acceptor ≤10 and H-bond donor ≤ 5 respectively (Muegge *et al*., 2001).

The results for drug-likeness evaluation for the seven phytocompounds identified from *Plectranthus amboinicus* were depicted in Table 5. Molecular weight and TPSA influences the rate of drug permeability or good absorption through biological barrier. Higher the molecular weight and TPSA, the permeability of a drug molecule lowers and vice versa. Even though the molecular weight of a drug plays an important role in the drug oral bioavailability, the phytocompounds falls in line with the cut-off mark set for all the rules which proves it as a good oral compound. TPSA is associated with the bioavailability of compound, if the TPSA value is < 140Å, the compound can be easily absorbed in the intestine thereby indicating its excellent oral bioavailabilty (Yang *et al*., 2020). TPSA of the selected phytocompounds were within the limits prescribed by the rules. The stereo-specificity of the drug molecule is a property of number of rotatable bonds and the results are in good agreement (≤10) with all the phtyocompounds. The oral bioavailability of phytocompounds with good membrane permeability as well as hydrophobicity of drug molecules is indicated by the Log P, TPSA, MW, HBA, and HBD values. Lipophilicity (Log P) plays a vital role by affecting the absorption of a drug molecule in the body. If the log P value is higher, the absorption rate will be lower and vice versa. In the present study all the phytocompounds falls in line with the standard limit prescribed for each rule and thereby indicates the increased absorption rate. Similarly the number of hydrogen bond donars and acceptors should be within the acceptable range, if it exceeds, the capability of the drug molecule to cross the cell membrane will be affected. The phytocompounds obeys the acceptable range and thereby has the ability to cross the cell membrane.

As a result of the drug-likeness investigation, the phytocompounds met the requirements of the Lipinski, Ghose, Veber, Egan, and Muegge guidelines, and they are expected to be orally bioavailable. These preliminary findings pave the way for more effective and selective anticancer medicines to be developed.

Table 5. Drug-likeness properties of the selected phytocompounds

| S. No | Compound | MW | HA | RB | HBA | HBD | MR | TPSA | XLOGP3 | WLOGP | MLOGP | Lipinski violation | Ghose violation | Veber violation | Egan violation | Muegge violation |
|---|---|---|---|---|---|---|---|---|---|---|---|---|---|---|---|---|
| 1 | Carvacrol | 150.22 | 11 | 1 | 1 | 1 | 48.01 | 20.23 | 3.49 | 2.82 | 2.76 | 0 | 0 | 0 | 0 | 0 |
| 2 | Cineole | 154.25 | 11 | 0 | 1 | 0 | 47.12 | 9.23 | 2.74 | 2.74 | 2.45 | 0 | 0 | 0 | 0 | 0 |
| 3 | Limonene | 136.23 | 10 | 1 | 0 | 0 | 47.12 | 0.00 | 4.57 | 3.31 | 3.27 | 0 | 0 | 0 | 0 | 0 |
| 4 | Pinene | 136.23 | 10 | 0 | 0 | 0 | 45.22 | 0.00 | 2.55 | 3.14 | 4.29 | 0 | 0 | 0 | 0 | 0 |
| 5 | Syringic acid | 198.17 | 14 | 3 | 5 | 2 | 48.41 | 75.99 | 1.04 | 1.11 | 0.49 | 0 | 0 | 0 | 0 | 0 |
| 6 | Thymol | 150.22 | 11 | 1 | 1 | 1 | 48.01 | 20.23 | 3.30 | 2.82 | 2.76 | 0 | 0 | 0 | 0 | 0 |
| 7 | Vanillin | 152.15 | 11 | 2 | 3 | 1 | 40.34 | 46.53 | 1.21 | 1.21 | 0.51 | 0 | 0 | 0 | 0 | 0 |

MW – Molecular Weight, HA – Hydrogen Atoms, RB- Rotatable Bonds, HBA – Hydrogen Bond Acceptors, HBD - Hydrogen Bond Donars, MR-Molecular Refractivity, TPSA –Total Polar Surface Area

The key characteristics for drug design and discovery in pharmaceutical research include pharmacokinetic and pharmacological aspects such as absorption, distribution, metabolism, excretion, and toxicity (ADMET), which serve in directing the preliminary evaluation of *in vivo* efficacy and drug safety. The degree of biological activity of a drug towards its target protein, as well as its adverse effects, is strongly influenced by its pharmacokinetic qualities. It also aids in determining whether the compounds or ligands have desirable qualities such as oral administration, absorption, etc., in order to avoid late-stage failure (Chandrasekaran *et al*., 2018 and Pricopie *et al*., 2020). Hence ADMET properties play a significant role in drug filtering which is carried out in evaluating the drug-likeness properties.

Among the ADMET properties, permeability, or a drug's capacity to pass through the human gastrointestinal tract, is a critical element in determining human intestinal absorption. High throughput screening methods were employed to examine the permeability of drug-like compounds using Caco-2 (adenocarcinoma cells originating from the colon), intestinal absorption (human), MDCK (Madin-Darby Canin Kidney) cell permeability, and skin permeability. The results of ADMET properties for the phytocompounds from *P. amboinicus* leaf extract were depicted in Table 6. Caco-2 cells are also known to express transporter and efflux proteins and conjugation enzymes that are universal pathways for transcellular incoming and metabolic change of foreign substances (Pham-The *et al*., 2013 and Oltra-Noguera *et al*., 2015). Caco-2 permeability results are interpreted based on the apparent permeability value (Papp) where, $P_{app}<1x10^{-6}$ cm/s indicate poor permeability, $P_{app}>10x10^{-6}$ cm/s indicate high and complete permeability, moderate permeability range for $1x10^{-6}$cm/s $<P_{app}<$ $10x10^{-6}$ cm/s which is compared with resultant value (Artursson and Karlsson, 1991). The Caco-2 cell permeability values ranges from 1.88-3.80cm/sec indicating the moderate permeability of the phytocompounds in the intestine. Human intestinal absorption determines the oral absorption of the drug from the intestine into the blood stream. However, greater the half life a of drug it could stay longer in the body and its potentiality is high, hence the

Table 6. – Pharmacokinetic properties of selected the phytocompounds

| S.No | PHARMACOKINETIC PROPERTIES | | Carvacrol | Cineole | Limonene | Pinene | Syringic acid | Thymol | Vanillin |
|---|---|---|---|---|---|---|---|---|---|
| 1 | ABSORPTION | Human Intestinal Absorption (HIA %) | 100 | 100 | 100 | 100 | 82.03 | 100 | 93.05 |
| | | Caco-2 Cell Permeability (cm/sec) | 3.80 | 2.87 | 2.36 | 2.23 | 1.88 | 3.80 | 1.95 |
| | | MDCK Cell Permeability (nm/sec) | 87.33 | 78.91 | 238.43 | 314.46 | 29.70 | 87.33 | 78.43 |
| | | Skin Permeability (log Kp, cm/hour) | -1.05 | -1.63 | -0.83 | -1.62 | -2.31 | -1.653 | -2.06 |
| 2 | BIOAVAILABILITY | Buffer Solubility (mg/l) | 903.91 | 832.99 | 14.06 | 51.95 | 25838 | 903.91 | 33.53 |
| | | Pure Water Solubility (mg/l) | 180.95 | 672.02 | 100.69 | 118.27 | 17371.2 | 180.95 | 2715.44 |
| 3 | DISTRIBUTION | Plasma Protein Binding (%) | 100 | 100 | 100 | 100 | 69.77 | 100 | 63.14 |
| | | Blood Brain Barrier Penetration | 6.39 | 1.29 | 8.27 | 4.87 | 0.54 | 6.39 | 0.56 |
| 4 | METABOLISM | CYP_1A2 Inhibitor | No | No | No | No | No | No | No |
| | | CYP_2C19_inhibitior | Yes | No | Yes | No | No | Yes | Yes |
| | | CYP_2C9_inhibitior | Yes | Yes | Yes | Yes | Yes | Yes | Yes |
| | | CYP_2D6_inhibitior | No | No | No | No | No | No | No |
| | | CYP_3A4_inhibitior | Yes | Yes | No | Yes | Yes | Yes | Yes |
| 5 | EXCRETION | Total Clearance (log ml/min/kg) | 0.207 | 1.009 | 0.213 | 0.066 | 0.646 | 0.211 | 0.601 |
| 6 | TOXICITY | AMES Toxicity | NM | NM | NM | NM | NM | NM | NM |
| | | hERG_inhibition | Low risk | Medium risk | Medium risk | Medium risk | Low risk | Low risk | Low risk |
| | | Mouse Carcinogen | Negative | Negative | Negative | Negative | Negative | Negative | Negative |
| | | Oral Rat Acute Toxicity ($LD_{50}$) | 2.074 | 2.01 | 1.88 | 1.762 | 2.157 | 2.074 | 1.937 |

half life determines the drug dosage. When it comes to intestinal absorption in humans, anything less than 30% is considered poorly absorbed. In the present study, all the phytocompounds exhibited good HIA which ranges from 82.03-100% and suggests its absorption in the intestine. If the value of log Kp is larger than -2.5 in terms of skin permeability, the phytocompound is regarded to have relatively poor skin permeability (Ntie-Kang *et al*., 2013). All the phytocompounds lies within the standard range indicating good skin permeability nature. MDCK cell permeability assay is a valuable tool to evaluate intestine or CNS (central nervous system) permeability and the suitability of the compound for oral administration. The Madin-Darby Canine Kidney (MDCK) cell line is commonly employed as an epithelial cell model in oral absorption research because it expresses transporter proteins but only extremely low amounts of metabolising enzymes (Veber *et al*., 2002). In the present study, MDCK cell absorption ranged from 29.70 to 314.45nm/sec and it was evidenced that all the phytocompounds had apparent MDCK cell permeability which falls within the recommended range of 25 - 500 $nms^{-1}$ (Ntie-Kang *et al*., 2013).

As a result, appropriate values of the number of rotatable bonds and molecular refractivity imply satisfactory intestinal absorption and oral bioavailability of the phytocompounds (Ibrahim *et al*., 2020). The bioavailability of a phytocompound is determined by the absorption and first-pass metabolism processes in the liver (Van de Waterbeemd *et al*., 2003). Aqueous solubility is an important physicochemical parameter in drug discovery as it reflects the bioavailability of the phytocompound. Formulation and course of administration, particularly oral dosing, are exigent for poorly soluble drugs, since absorption of compound from the gastrointestinal tract is limited. Hence, solubility influences ADME properties, because precipitation of the phytocompound will make it unavailable. In the same line, the absorption and solubility levels of a phytocompound following oral administration represent human intestinal absorption and drug likeliness respectively. For aqueous solubility, the solubility level of a compound is rated as good, optimal and too soluble. The phytocompounds tested in the study possessed good solubility level.

ADME infers the distribution of drugs throughout the body. Blood brain barrier and plasma protein binding are the vital factors for drugs which target the brain cells primarily and across the membrane respectively. The extent to which a drug interacts to the proteins in blood plasma can jeopardise its effectiveness. It is significant to note that drug binding to plasma proteins such as human serum albumin, lipoprotein, glycoprotein, α, β, and γ and globulins reduces the amount of drug in blood circulation, and so the less bound a drug is, the better it can transit cell membranes or diffuse. The plasma protein functions as a drug-extracting pump, which necessitates the use of energy and takes place in the cell membrane's pores. They are expressed in large level in liver, kidney, pancreas, adrenal cortex and colon thereby suggesting its role in secretion. In tumour tissues, expression of plasma proteins in higher level is correlated with multiple drug resistance (Gómez *et al*., 2002). The phytocompounds exhibited good plasma protein values in the range of 63.14 - 100%. To assess the distribution of phytocompounds, the blood–brain barrier membrane permeability (logBB) was utilised. The Central Nervous System is protected by the separation of brain tissues from the blood stream through blood brain barrier which is formed by brain endothelium. Blood brain barrier prevents the entry of large (100%) and small (98%) molecules and allows only the water and lipid soluble and selectively transport molecules such as plasma glycoprotein and glucose transporters into the central nervous system (Wang *et al*., 2018). If logBB is greater than 0.3, the phytocompounds were able to easily penetrate the blood–brain barrier membrane, and if logBB is less than -1, phytocompounds are unable to enter the blood–brain barrier membrane (Pires *et al*., 2015). The phytocompounds in this investigation had blood brain barrier penetration values in the range of 0.54 - 8.27, which is within the standard limit, indicating that they can easily penetrate.

The metabolism of drugs is a complicated process where they are structurally modified to distinct molecules by various enzymes. In drug development, metabolism plays an important role and its impact on pharmacodynamics, pharmacokinetics and safety should be considered. Drug delivery to a particular site may get affected if the gastrointestinal absorption and metabolism in liver gets changed or affected, hence these should be considered

as a crucial factor. The enzyme, Cytochrome P450 (CYP) which is present in liver and intestine plays an important role in drug-drug interaction and also in drug metabolism. These enzymes can be activated or inhibited by various substrates and drugs, resulting in pharmacological interactions that induce toxicity or a loss in therapeutic benefits (Issa *et al*., 2017). The drugs orally absorbed travel through the blood and enters liver where they get degraded by CYP450 and further exerted. However, if a phytocompound acts as a substrate for more than a single CYP450 enzyme then the compound is said to be metabolised by the respective CYP450 enzyme (Li, 2001 and Guengerich *et al*., 1999). The CYP enzyme specifically the isoforms 1A2, 2C9, 2C19, 2D6 and 3A4 were responsible for 90% of oxidative metabolic reaction and also the substrate for the therapeutic molecule (Williams *et al*., 2003). In the metabolism section all the phytocompounds were not inhibitory to CYP-1A2 and CYP-2D and no severe drug interaction toxicity was caused in the liver, whereas carvacrol, limonene and thymol showed inhibition against CYP-2C19 and limonene alone showed no inhibitory effect against CYP-3A4. All the phytocompounds showed inhibition against CYP-2C9 stating the responsibility for drug clearance.

Total clearance is a key pharmacokinetic parameter which encompasses metabolism and excretion of a drug. It controls the half life, bioavailability, frequency and maintain the dosing concentrations of a drug (Berellini *et al*., 2012). Results revealed that all the identified phytocompounds had positive total clearance values and can be easily eliminated.

Toxicity is the measure to which a compound can damage an organism or its organs such as cells and tissues, and is the most reason for drug development failure in the late stages (Lagorce *et al*., 2017). In the present study toxicity properties such as AMES toxicity, mouse carcinogenicity, hERG-inhibition, oral rat acute toxicity ($LD_{50}$) and minnow toxicity were tested. The Ames test is a mutagenicity assay that uses *Salmonella typhimurium* to determine whether phytocompounds are carcinogenic. All the phytocompounds displayed negative AMES toxicity test depicting the nonmutagenic effect. hERG (human- ether- a-go-go-related gene) is considered as an important model since the inhibition of the hERG potassium channel in human may end in QT interval prolongation and

results in severe cardiac side effects, which is a foremost problem in clinical studies of drug (Wang *et al*., 2012). The hERG potassium channel emerges to be the molecular target accountable for cardiac toxicity of an extensive range of therapeutic drugs and best known for its role in the electrical activity of the heart which regulates the heart beat (Vandenberg *et al*., 2001). The phytocompounds evaluated on hERG activity possess low to medium risk for hERG-inhibition and thereby reduce the entry of cardiotoxic drugs.

Moreover, the toxicological endpoints posing greatest risk for human health were acute oral toxicity and carcinogenicity. The lethal dose ($LD_{50}$) is a standard measurement of acute toxicity used to evaluate the relative toxicity of phytocompounds. Acute toxicity illustrates the adverse effects of a compound that transpire within a short time after exposure and is an essential marker of the drug safety assessment executed during the initial stages of toxicological research. Results revealed that the tested phytocompounds were non-carcinogenic to mouse, possess less toxicity and lethality to the different model organisms.

### 4.3.3 Receptors preparation and molecular docking

The identified ligands namely carvacrol, cineole, limonene, pinene, syringic acid, thymol and vanillin from the leaf extract of *P. ambionicus* and docked with the protein targets using Auto Dock Vina (Version 4). The binding affinity of the ligands with the apoptotic regulatory protein target molecules are presented in Table 7.

Table 7. Docking score of phytocompounds against apoptotic receptor proteins

| Ligands | Apoptotic Regulator Target Proteins | | | | | | |
|---|---|---|---|---|---|---|---|
| | **3MK8** | **3PK1** | **4IDT** | **4ZBF** | **5FMI** | **5LAY** | **5MW7** |
| Carvacrol | **-5.7** | **-6.0** | **-6.4** | **-6.7** | **-5.5** | **-6.1** | -5.3 |
| Cineole | -5.2 | **-4.8** | -6.1 | -6.1 | -5.2 | -5.4 | -4.8 |
| Limonene | -5.2 | -5.5 | -6.1 | -6.3 | -5.4 | -5.7 | **-4.5** |
| Pinene | -5.1 | -5.3 | **-5.2** | -6.3 | -5.3 | -5.4 | **-4.5** |
| Syringic acid | -5.5 | -5.4 | -5.9 | **-5.4** | **-5.0** | -5.9 | **-5.6** |
| Thymol | -5.6 | -5.6 | -6.3 | -6.3 | **-5.5** | -5.8 | -5.0 |
| Vanillin | **-5.0** | -5.2 | -5.6 | -5.6 | -5.1 | **-5.3** | **-5.6** |

The docking interactions of ligands with 3MK8 target molecule demonstrate binding affinity ranging from -5.0 kcal/mol to -5.7kcal/mol, where the highest binding affinity of -5.7 kcal/mol and the lowest binding affinity of -5.0 kcal/mol were recorded in carvacrol and vanillin respectively. The docking interaction of ligands with 3PK1 target molecule exhibited the binding affinity from -4.8kcal/mol to -6.0kcal/mol, where carvacrol shows highest binding affinity (-6.0 kcal/mol) and cineole with lowest binding affinity of -4.8 kcal/mol. The docking interactions of ligands with the target molecule 4IDT revealed binding affinity from -5.2 kcal/mol to -6.4 kcal/mol. Carvacrol and pinene exhibited highest and lowest binding affinity score of -6.4 kcal/mol and -5.2 kcal/mol respectively. The docking interaction of ligands with 4ZBF target molecule revealed the binding affinity from -5.4 kcal/mol to -6.7 kcal/mol where carvacrol and syringic acid exhibited highest (-6.7 kcal/mol) and lowest (-4.8 kcal/mol) binding affinity. The docking interaction of ligands with 5FMI target protein exhibited binding affinity ranging from -5.5 kcal/mol to -5.0 kcal/mol where the highest binding affinity is depicted by carvacrol and thymol with -5.5 kcal/mol and the lowest binding affinity by syringic acid (-5.0 kcal/mol). The docking interaction of ligands with the target protein 5LAY exhibited binding affinity ranging from -6.1 kcal/mol to -5.3 kcal/mol with carvacrol (-6.1 kcal/mol) and vanillin (-5.3 kcal/mol) revealing highest and lowest binding affinity respectively. The docking interaction of ligands with 5MW7 target protein exhibited binding affinity ranging from -5.6 kcal/mol to -4.5 kcal/mol. The highest binding affinity is shown by syringic acid and vanillin (-5.6 kcal/mol) and the lowest binding affinity is shown by limonene and pinene (-4.5 kcal/mol). The top scored phytocompounds with the receptors were further selected for the docking complex interactions and they were depicted in Table 8.

Phenolic anticancer compounds namely quercetin, gallic acid, sinapic acid, vanillic acid, 4-hydroxy-3-methoxy benzoic acid, p-coumaric acid, m-coumaric acid, 4-hydroxy-3-methoxy cinnamic acid, caffeic acid, and syringic acid from *Moringa oleifera* possess a good binding energy values in the range of -5.6 to -7.8kcal/mol. These phenolic acids may reduces tumour initiation by suppressing genotoxic chemicals, mutagen-transforming enzyme activity and

Table 8. Molecular interaction of top scored ligands with apoptotic regulator proteins

| S. No | Docking Complex ( Target-Ligand) | Docking Score (-kcal/mol) | No of H Bonds | No of Alkyl Bonds | Residues Involved in Alkyl Interactions and Hydrogen Bonding |
|---|---|---|---|---|---|
| 1 | 3MK8- Carvacrol | -5.7 | 1 | 5 | Val16,His20,Val216,His224,Phe319,Asn223*, |
| 2 | 3PK1- Carvacrol | -6.0 | - | 4 | Leu232,Phe273,Lys276,His277 |
| 3 | 4IDT- Carvacrol | -6.4 | - | 5 | Leu406,Val414,Ala427,Leu472,Leu522 |
| 4 | 4ZBF- Carvacrol | -6.7 | - | 10 | Met231,Leu235,Val246,Val249,Met250,Val253,Val274, Phe270,Leu290,Ile294 |
| 5 | 5FMI- Carvacrol | -5.5 | 1 | 5 | #Tyr108,Arg156,Phe157,Phe161,His165 |
| 6 | 5FMI- Thymol | -5.5 | - | 5 | Tyr108,Phe157,Phe161,His164,His165 |
| 7 | 5LAY- Carvacrol | -6.1 | 1 | 5 | Lys31,Pro32,Leu33,Arg65,Tyr67*,Leu85 |
| 8 | 5MW7- Syringic Acid | -5.6 | 5 | 1 | Arg114*,Asp176*,Cys198,Asp199*,Tyr202*,Ser204* |
| 9 | 5MW7- Vanillin | -5.6 | 5 | 1 | Arg114*,Pro174*,Tyr202*,Tyr203, Srer204*,Gln225* |

modulating enzymes such as heme-containing phase I and carcinogen-detoxifying phase II enzymes (Mumtaz *et al*., 2021). Flavonoids from *Plectranthus amboinicus* possess good anticancer activity with 50% inhibitory activity using its extract and further confirmed by *in silico* docking with various cancer target proteins (Manurung *et al*., 2020).

The interaction of carvacrol with 3MK8 is favoured by the formation of one hydrogen bond and five alkyl bonds with Val 16, His20, Val216, His224, Phe319, Asn223 (Fig. 14).

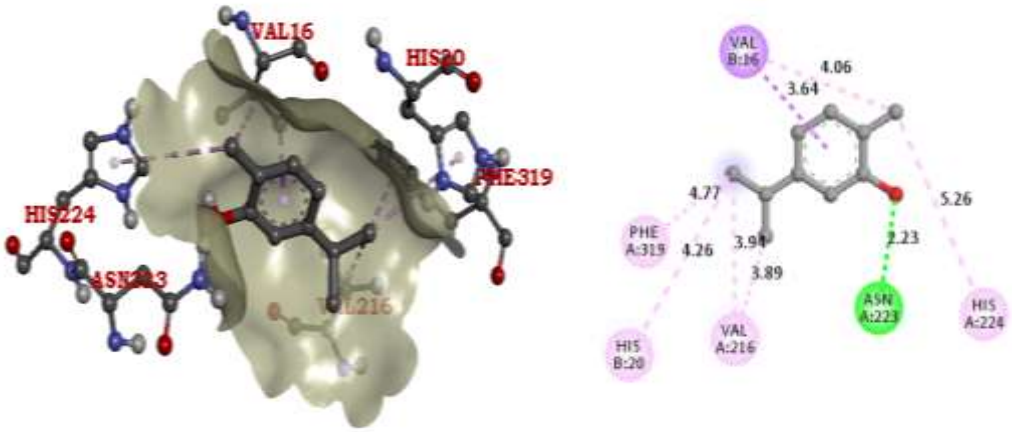


Fig. 14 3MK8-Carvacrol Docking Pose and Interaction Plot (-5.7 kcal/mol)

The interaction of carvacrol with 3PK1 is favoured by the formation of four alkyl bonds with Leu232, Phe273, Lys276 and His277 (Fig. 15).

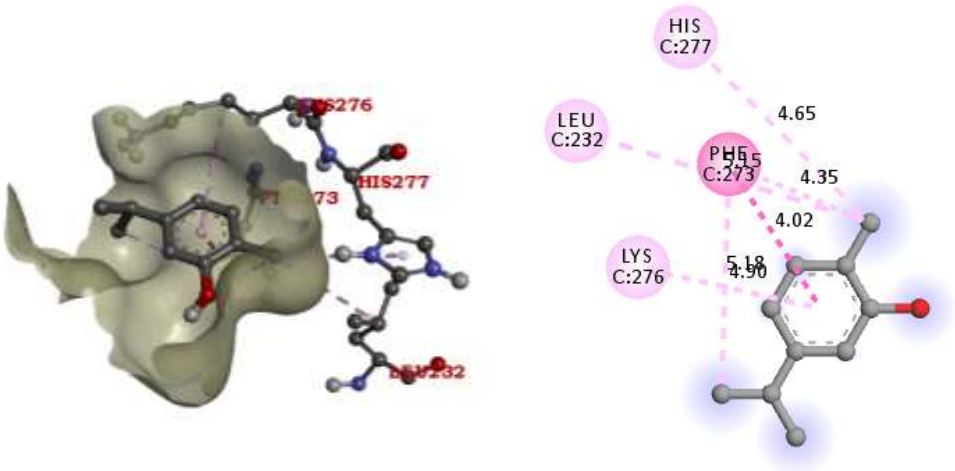


Fig.15 3PK1-Carvacrol Docking Pose and Interaction Plot (-6.0 Kcal/mol)

The interaction of carvacrol with 4IDT is favoured by the formation of five alkyl bonds with Leu406, Val414, Ala427, Leu472 and Le522 (Fig. 16).

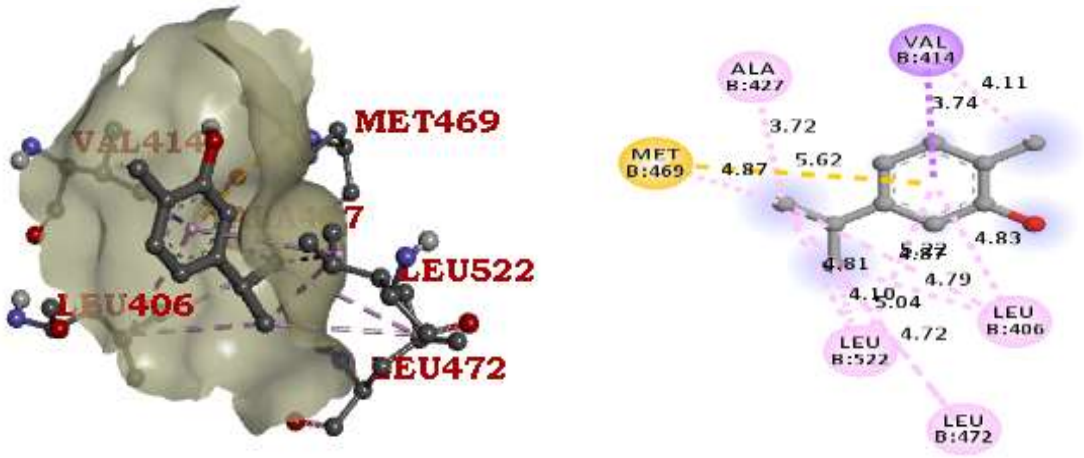


Fig.16 4IDT-Carvacrol Docking Pose and Interaction Plot (-6.4 Kcal/mol)

The interaction of carvacrol with 4ZBF is favoured by the formation of ten alkyl bonds with Met231, Leu235, Val246, Val249, Met250, Val253, Val274, Phe270, Leu290 and Ile294 (Fig. 17).

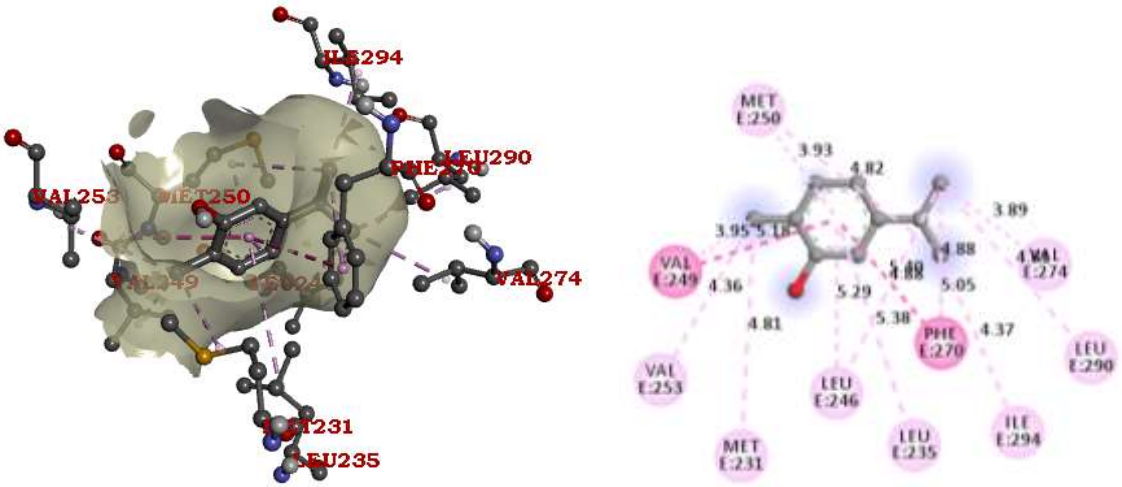


Fig.17 4ZBF-Carvacrol Docking Pose and Interaction Plot (-6.7 Kcal/mol)

The interaction of carvacrol with 5FMI is favoured by the formation of one hydrogen bond and five alkyl bonds with Tyr108, Arg156, Phe157, Phe161 and His165 (Fig. 18).

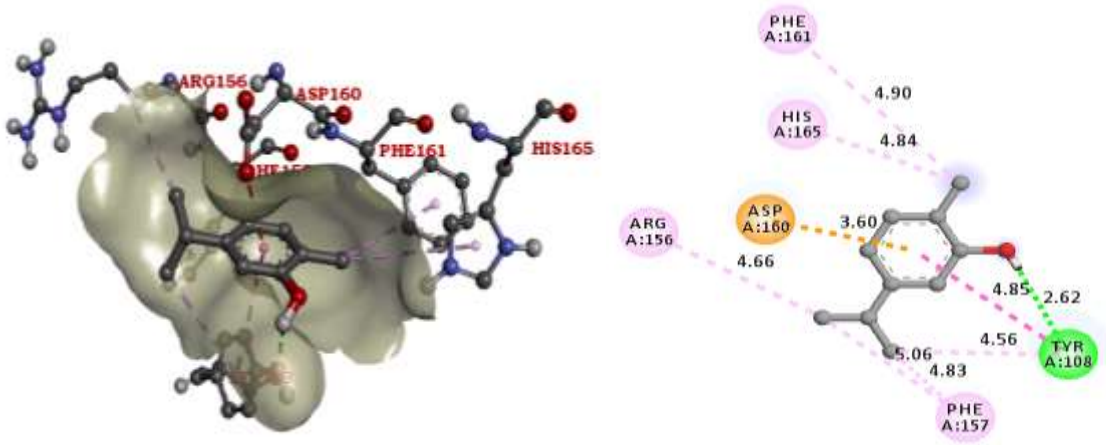


Fig. 18 5FMI-Carvacrol Docking Pose and Interaction Plot (-5.5 Kcal/mol)

The interaction of thymol with 5FMI is favoured by the formation of five alkyl bonds with Tyr108, Phe157, Phe161, His164 and His165 (Fig. 19).

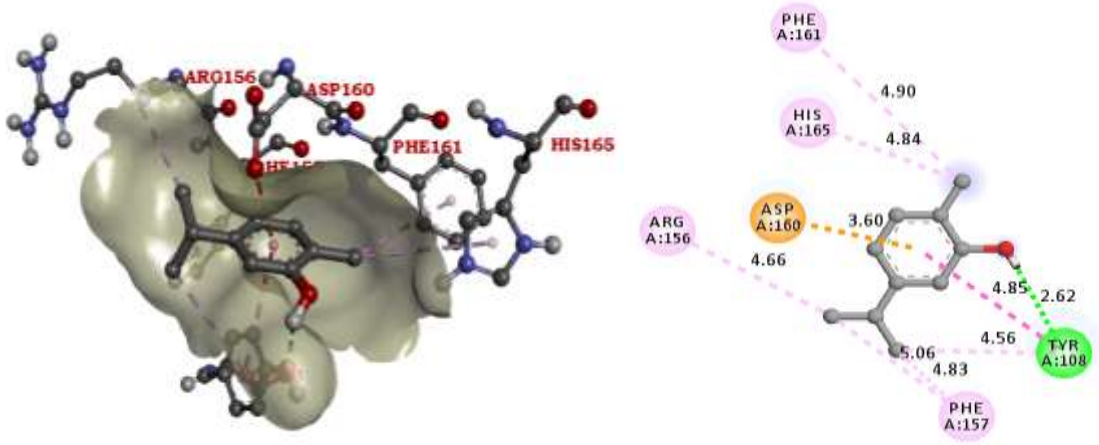


Fig. 19 5FMI-Thymol Docking Pose and Interaction Plot (-5.5 Kcal/mol)

The interaction of carvacrol with 5LAY is favoured by the formation of one hydrogen bond and five alkyl bonds with Lys31, Pro32, Leu33, Arg65, Tyr67, Leu85 (Fig. 20).

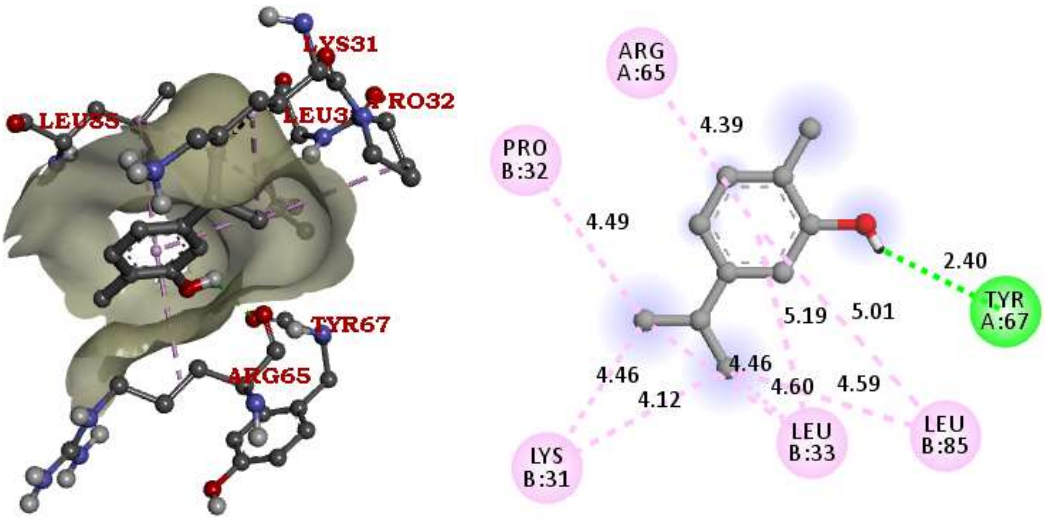


Fig. 20 5LAY-Carvacrol Docking Pose and Interaction Plot (-6.1 Kcal/mol)

The interaction of syringic acid with 5MW7 is favoured by the formation of five hydrogen bonds and one alkyl bond in Arg114, Asp176, Cys198, Asp199, Tyr202 and Ser204 (Fig. 21).

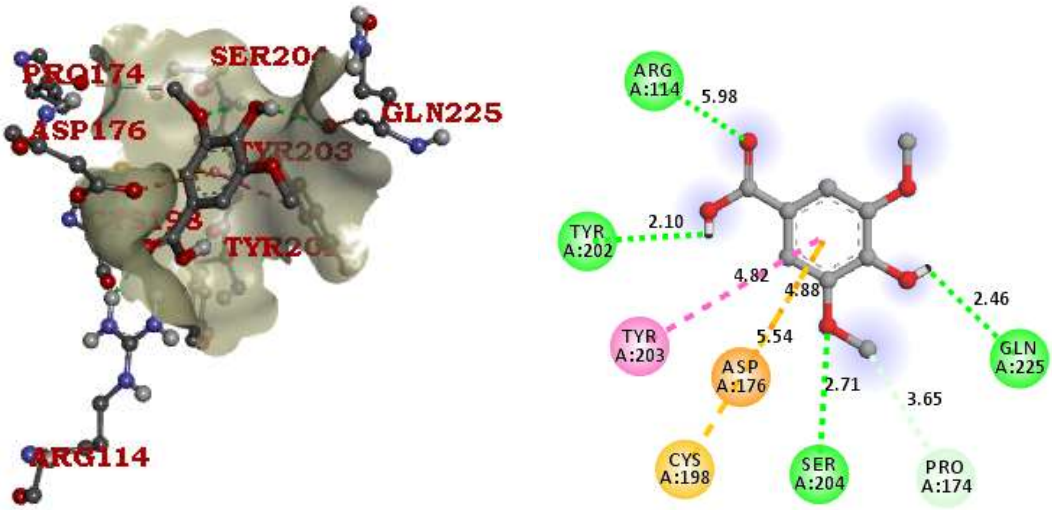


Fig. 21 5MW7-Syringic acid Docking Pose and Interaction Plot (-5.6 Kcal/mol)

The interaction of vanillin with 5MW7 is favoured by the formation of five hydrogen bonds and one alkyl bond in Arg114, Pro174, Tyr202, Tyr203, Ser204 and Gln225 (Fig. 22).

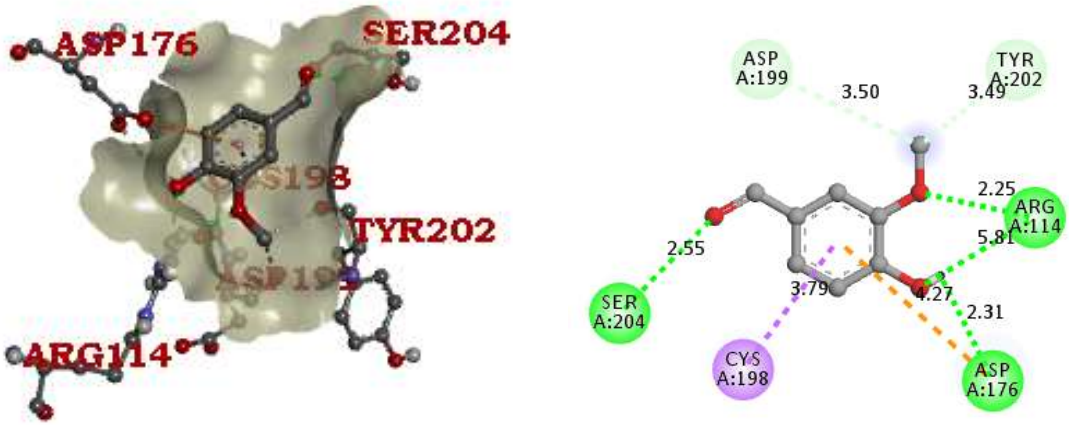


Fig. 22 5MW7-Vanillin Docking Pose and Interaction Plot (-5.6 Kcal/mol)

### 4.3.4 Density Functional Theory Analysis

Density Functional Theory is a quantum mechanical approach which explains both structural and electronic properties of compounds with accuracy through B3LYP/6-31G* level. In the present study, the electronic distribution of the docked phytocompounds namely carvacrol, cineole, limonene, pinene, syringic acid, thymol and vanillin were theoretically established through orbital energy calculations. This may help to frame an idea of protein-ligand interactions and their usefulness in exploring the inhibition potential of phytocompounds. The high and low level of electron density regions in the phytocompounds can be computed by highest occupied molecular orbital energies (HOMO) and lowest occupied molecular orbital energies (LUMO). The DFT calculations of the seven phytocompounds obtained from the extract of *Plectranthus ambionicus* is summarized in the Table 9 and Fig. 23a to 23g illustrates the HUMO and LUMO models of the phytocompounds. The positive and the negative phase are indicated by green and red colour respectively.

Table 9. DFT indices of the selected phytocompounds

| Phyto compounds | HOMO | LUMO | Energy Gap | Ionization potential (IE) (eV) | Electron affinity (EA) (eV) | Electro negativity ($\chi$) (eV) | Electro chemical potential ($\mu$) (eV) | Hardness ($\eta$) (eV) | Softness ($\sigma$) (eV) | Electro philicity Index ($\omega$) |
|---|---|---|---|---|---|---|---|---|---|---|
| Carvacrol | -0.2098 | 0.0112 | -0.2211 | 0.2098 | -0.0112 | 0.0993 | -0.0993 | 0.1105 | 9.0497 | 0.0446 |
| Cineole | -0.2365 | 0.0920 | -0.3285 | 0.2365 | -0.0920 | 0.0722 | -0.0722 | 0.1642 | 6.0869 | 0.0159 |
| Limonene | -0.2236 | 0.0288 | -0.2525 | 0.2236 | -0.0288 | 0.0974 | -0.0974 | 0.1262 | 7.9239 | 0.0375 |
| Pinene | -0.2177 | 0.0323 | -0.5201 | 0.2177 | -0.0323 | 0.0927 | -0.0927 | 0.12507 | 7.9955 | 0.0343 |
| Syringic acid | -0.2216 | -0.0373 | -0.1843 | 0.2216 | 0.0373 | 0.1294 | -0.1294 | 0.0921 | 10.8477 | 0.0909 |
| Thymol | -0.2154 | 0.0083 | -0.2238 | 0.2154 | -0.0083 | 0.1035 | -0.1035 | 0.1119 | 8.9365 | 0.0478 |
| Vanillin | -0.2148 | -0.0488 | -0.1660 | 0.2148 | 0.0488 | 0.1318 | -0.1318 | 0.083 | 12.0481 | 0.1047 |

**HUMO**

a. Syringic acid

b. Thymol

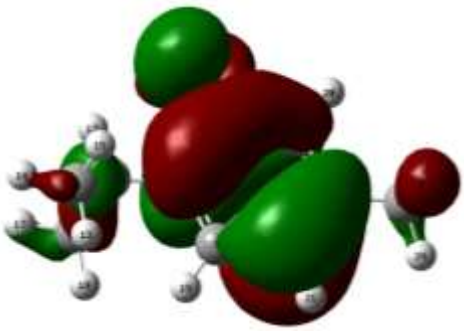

c. Carvacrol

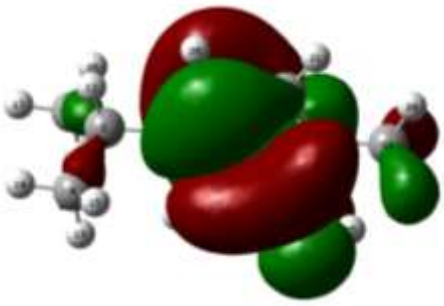

d. Limnonene

**LUMO**

a. Syringic acid

b. Thymol

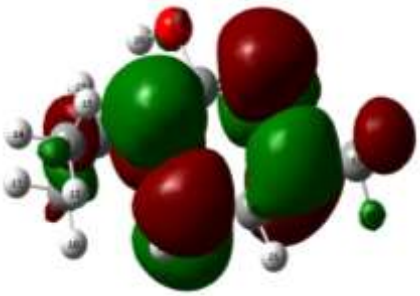

c. Carvacrol

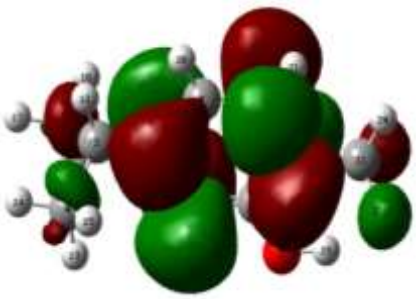

d. Limnonene

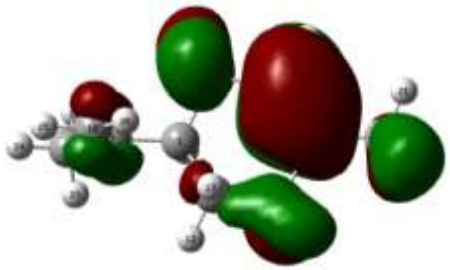

e. Cineole

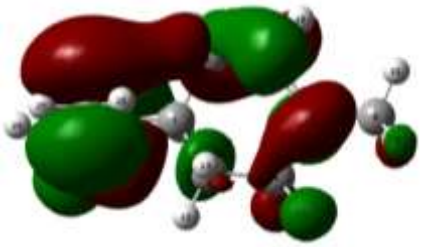

e. Cineole

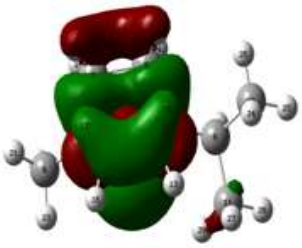

f. Pinene

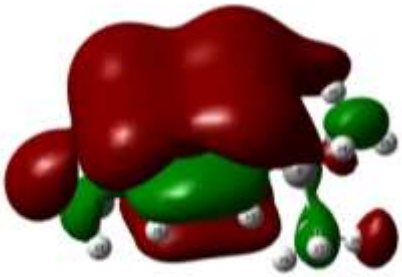

f. Pinene

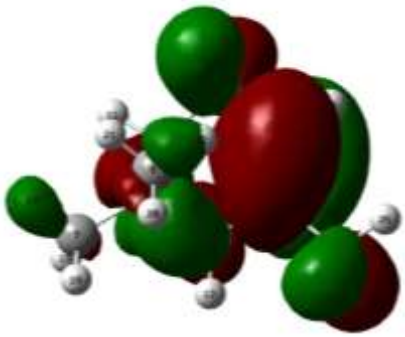

g. Vanillin

g. Vanillin

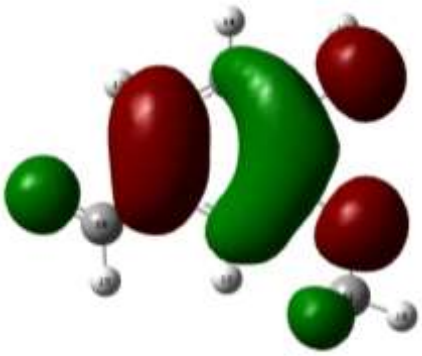

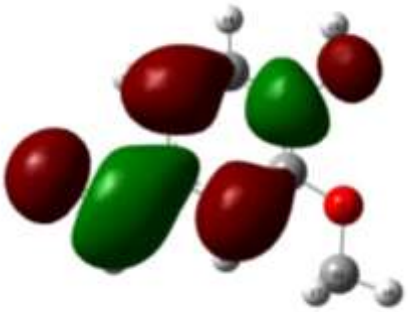

Fig. 23(a-g) HUMO and LUMO models of the selected phytocompounds

The localization of HOMO and LUMO orbitals is vital since the free electrons from HOMO helps in the transfer of charges in protein-ligand complex formation. Moreover, the HOMO and LUMO of a molecule plays an important role in revealing the intermolecular interactions which takes place between the HOMO of a drug and LUMO of a receptor and as well as between HOMO of a receptor and LUMO of a drug. The energy gap between the interacting orbitals is used to calculate the stability of the interactions. The development of complex interaction stability and strongest binding ability with the receptor is predicted by increasing HOMO and decreasing LUMO energies in the compounds. Furthermore, the electrostatic potential maps visibly display relative polarity, electrophilic and nucleophilic sites of a compound, which can be utilised to envisage the favourable sites on the compound that are involved in the formation of receptor interactions. The energy gap between HOMO and LUMO is a critical parameter for defining a chemical system's electrical conductivity and other molecular properties. Energy gap level also elucidates the chemical stability and reactivity of a molecule. HOMO – LUMO energy gap is large and small for the hard and small molecule respectively, which means the hardest molecule is less reactive and soft molecule is highly reactive. Also small energy gap is best for bonding and signifies the easy electronic transition.

From the above Table 9 it is evident that the selected phytocompounds namely vanillin (-0.166eV, 0.083eV and 12.0481eV), syringic acid (-0.18437eV, 0.0921eV and 10.8477 eV), carvacrol (-0.2211eV, 0.1105eV and 9.0497eV), thymol (-0.2238eV, 0.1119 eV and 8.9365 eV), pinene (-0.52014eV, 0.12507eV and 7.9955eV), limonene (-0.2525eV, 0.1262eV and 7.9239eV) and cineole (-0.32857eV, 0.164285eV and 6.0869eV) demonstrated more stability and biological activity as illustrated by less energy gap, low hardness and high softness.

When a molecule gains an additional amount of electron density from the environment, its energy stability is measured by the electrophilicity index (ω). It encompasses the electrophile's inclination to gain an additional amount of electron density, as determined by μ, and a molecule's resistance to exchanging

electron density with the environment, as determined by η. Thus, a good electrophile is a species characterised by a high |μ| value and a low η value. The electrophilicity scale allowed the classification of organic molecules as strong electrophiles with ω > 1.5eV, moderate electrophiles with 0.8 < ω < 1.5 eV and marginal electrophiles with ω < 0.8eV (Parr *et al.,* 1999 and Domingo *et al*., 2002). Results emanated from the study revealed that the electrophilicity index was in the limit of ω < 0.8 eV (Table 9) thereby depicting the identified phytocompounds as a marginal electrophiles in the biological activity. Thus the DFT analysis proves to be a valuable tool for predicting the biological activity of the phytocompounds and the HUMO-LUMO energy gaps reveals its stability index.

### 4.3.5 Bioactivity score prediction

The potency of a phytocompound is predicted on the basis of bioactivity score. The bioactivity score provides information on the binding cascade of compounds with various protein structures and is used to find new functional pharmaceuticals with improved binding selectivity profiles and fewer side effects. Drug ability likeliness properties of the phytocompounds were studied against GPCR ligands, ion channel modulators, kinase inhibitors, nuclear receptor ligands, protease inhibitors and enzyme inhibitors, and results were depicted as bioactivity scores in Table 10.

Table 10. Predicted bioactivity score of the phytocompounds

| Phyto compounds | Parameters of Bioactivity score | | | | | |
|---|---|---|---|---|---|---|
| | GPCR ligand | Ion channel modulator | Kinase inhibitor | Nuclear receptor ligand | Protease inhibitor | Enzyme inhibitor |
| Carvacrol | -1.02 | -0.51 | -1.15 | -0.70 | -1.25 | -0.56 |
| Cineole | -0.93 | -0.01 | -1.60 | -1.07 | -0.90 | -0.15 |
| Limonene | -0.91 | -0.27 | -2.01 | -0.34 | -1.38 | -0.21 |
| Pinene | -0.48 | -0.43 | -1.50 | -0.62 | -0.85 | -0.34 |
| Syringic acid | -0.65 | -0.28 | -0.69 | -0.44 | -0.82 | -0.15 |
| Thymol | -1.05 | -0.53 | -1.29 | -0.78 | -1.34 | -0.57 |
| Vanillin | -1.20 | -0.54 | -1.13 | -0.91 | -1.65 | -0.64 |

The bioactivity scores for the phytocompounds was interpreted as highly active (when the bioactivity score > 0.00), moderately active (when the bioactivity score lies between − 5.0 to 0.00) and no biological activity or inactive (when the bioactivity score < − 5.0) (Mishra *et al*., 2018). As seen from Table 10, the bioactivity score of the phytocompounds were between -5.0 and 0.0 which predicted moderate biological activity in all cases.

G-protein coupled receptors (GPCR) interfere with the surface of cancer cells and cause the surface proteins to lose receptor function, leading to the disruption of cell wall absorption and penetration, stop the nutrient supply and oxygen to cells. Phytocompounds present in the extract disrupts the cell function, interact with cancer cells and reduce its virulence and increase apoptosis and cytotoxicity (Campillo *et al*., 2019 and Thang *et al*., 2012). By blocking and opening ions on the cell wall surface, an ion channel modulator interferes with cancer cells ability to develop. They can impair the communication mechanism between cells and within cells thereby impede with protein synthesis and prevent the development of cancer cells (Burke *et al*., 2019).The antioxidants in *Chromolaena odorata* may inhibit cancer cell development by inhibiting cancer cell kinase enzyme, which catalyse protein phosphorylation and regulate various cellular functions for cancer cell survival and spread, including proliferation, cell cycle, apoptosis, motility, growth and differentiation (Cicenas *et al*., 2018). The nuclear receptors are significant pharmaceutical targets because they act as initiators of DNA transcription, regulate to produce lipophilic proteins and control homeostasis and inflammation (Weikum *et al.,* 2018). By preventing the proteolytic cleavage of protein precursors required by pathogens to produce disease, protease inhibitors can restrict the generation of infectious agents and viral replication, which can aggravate infection. This suggests that these protease inhibitors can protect patients with breast and colorectal cancer from subsequent infections (Patick *et al*., 1998). Furthermore, enzyme inhibitors in the phytocompounds *C. odorata* can bind with cancer cell metabolic enzymes, lessen the nutrient intake, restrain the enzyme-substrate complex formation, prevent catalytic processes, kill pathogens and improve metabolic imbalances. Also,

*C. odorata* was capable of balancing average cell growth and decrease the number of cancer cells (Lupien *et al*., 2019 and Robin *et al*., 2018).

Thus the molecular docking simulation, DFT analysis and the bioactivity score prediction demonstrated the promising apoptosis - modulating effect of the phytocompounds and validate them as a strong anticancer agent. Based on the results of *in silico* studies, the presence of phenolic acid, syringic acid the phytocompounds of interest was assessed in phase IV.

## PHASE IV

## 4.4 IDENTIFICATION OF BIOACTIVE PRINCIPLES IN *P. amboinicus* LEAF EXTRACT

Medicinal plants are employed in home remedies and as an ingredient in pharmaceutical sectors in developing countries. To ensure the reliability of active principles in the herbal products, it is necessary to isolate them and to assess its biological activities. Hence the present study was sculpted to characterize the presence of bioactive principles in the *Plectranthus amboinicus* leaf extract and further subjected to chromatography to identify the phytocompound of interest, syringic acid.

### 4.4.1 FT- IR analysis in the methanolic extract of *P. amboinicus*

The FT-IR spectrum of *P. amboinicus* was studied to identify the nature of functional groups present. The peaks and functional groups of the spectrum are depicted in Fig. 24. The spectrum revealed a strong and broad peak at 3859.56$cm^{-1}$ and 3346.50$cm^{-1}$ which is attributed to –OH and –NH stretching vibrations of hydroxyl and phenol groups respectively. The peaks at 2349.30$cm^{-1}$, 2308.79$cm^{-1}$ and 2137.13$cm^{-1}$ is attributed to –C≡C– stretching vibrations of alkyne groups. The peaks at 1641.42$cm^{-1}$ and 1544.98$cm^{-1}$ are indicative of strong C=C stretching. The peaks at 1367.53$cm^{-1}$ revealed C-H bending vibrations. The peaks at 1228.66$cm^{-1}$,1217.08$cm^{-1}$ and 1062.78$cm^{-1}$ represents the strong C-N stretching vibrations of amine groups. The peak at 680.87$cm^{-1}$ represents the C-H bending vibrations. Thus the FT-IR analysis suggests the

presence of different functional groups like hydroxyl, amines and alkynes in the methanolic extract of *P. amboinicus*.

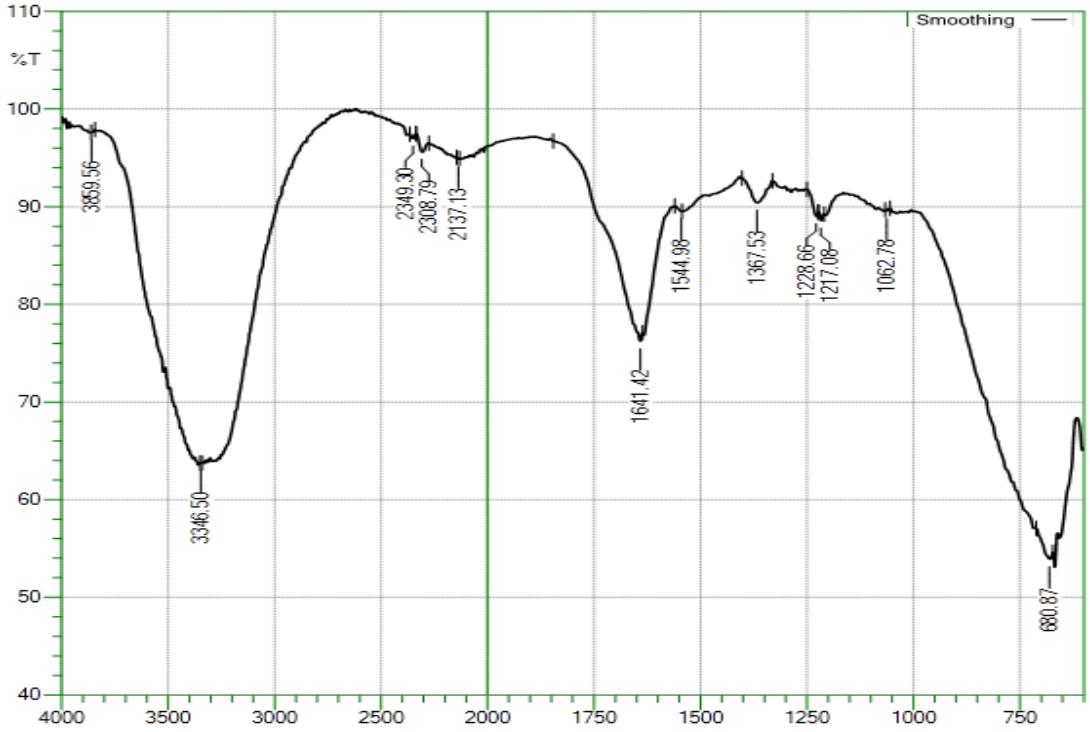


Fig. 24 FT-IR spectrum of methanolic extract of *P. amboinicus*

### 4.4.2 NMR analysis in the methanolic extract of *P. amboinicus*

The 1 H NMR spectra for the methanolic extract of *P. amboinicus* revealed the presence of carboxylic acid group (COOH) which was assigned by a singlet peak at δ9.2 and three aromatic protons of the acid resonated as multiplets from δ6.7 to δ6.9. Hydroxyl proton and methyl (-$OCH_3$) groups were resonated around δ3.5 to δ3.6 as multiplets. The peaks obtained from the *P. amboinicus* leaf extract was compared with the syringic acid of NIST library where 1H NMR spectrum revealed a peak at δ9.2, which is due to the presence of carboxylic acid group (COOH), the peak resonating at δ7.2, δ3.823 and δ3.8 represents the hydrogen, methyl and hydroxyl groups respectively (Fig. 25). From the NMR data, the results confirm the presence of syringic acid along with other compounds as comparable with NIST library.

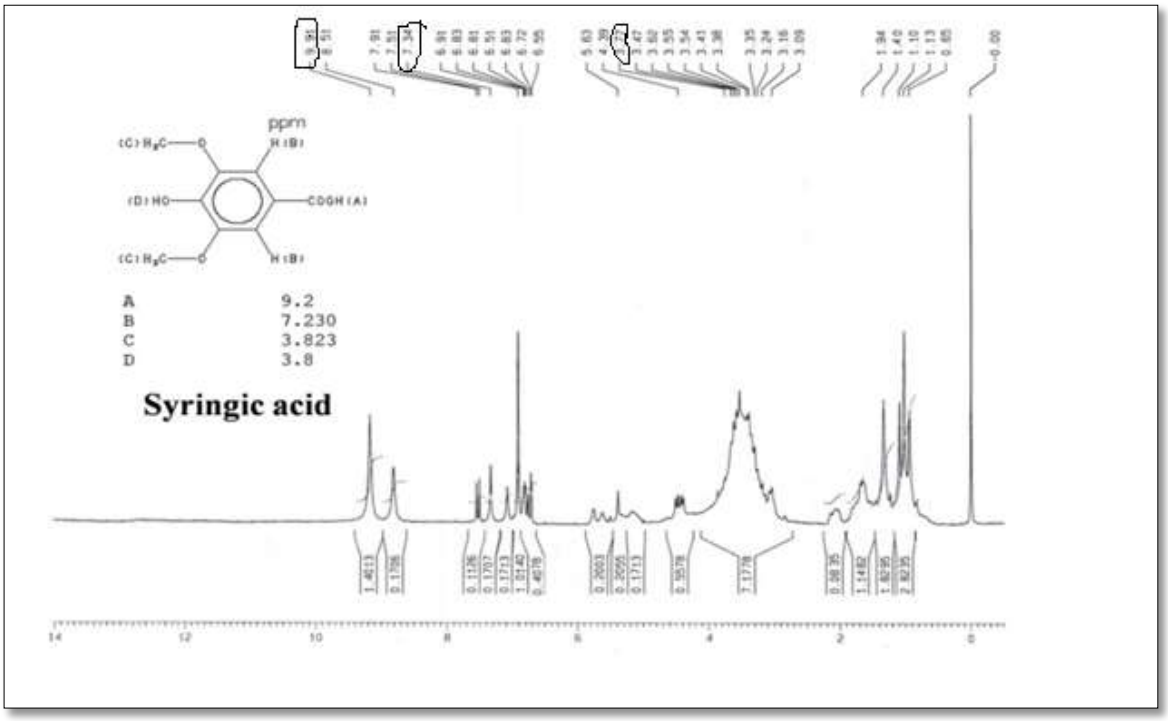


Fig. 25 NMR spectrum of methanolic extract of *P. amboinicus*

### 4.4.3 Syringic acid fraction extraction by bioassay-guided fractionation

A total of 8 fractions were collected finally, and the amount of phenol was estimated. The results revealed that fraction 4 proved to exhibit high amount of phenol (43.81µg/g) when compared with other fractions and hence it was further subjected to UV-Vis, HPLC and HPTLC analyses.

### 4.4.4 UV-Vis spectral analysis of the syringic acid fraction

The absorption spectra of fraction 4 revealed distinct peaks at 277nm and 463nm, which indicates the presence of phenolic compounds and their derivatives. Hence the isolated fraction was compared with the commercially available syringic acid which serves as standard and its absorption peak was noted as 287nm (Fig. 26). It was noticed that the absorption peak of fraction 4 coincides with the standard syringic acid and thus its presence was confirmed. Lattanzio (2013) reported that the phenolic compounds have its absorptive intensity at UV range which represents its characteristic nature.

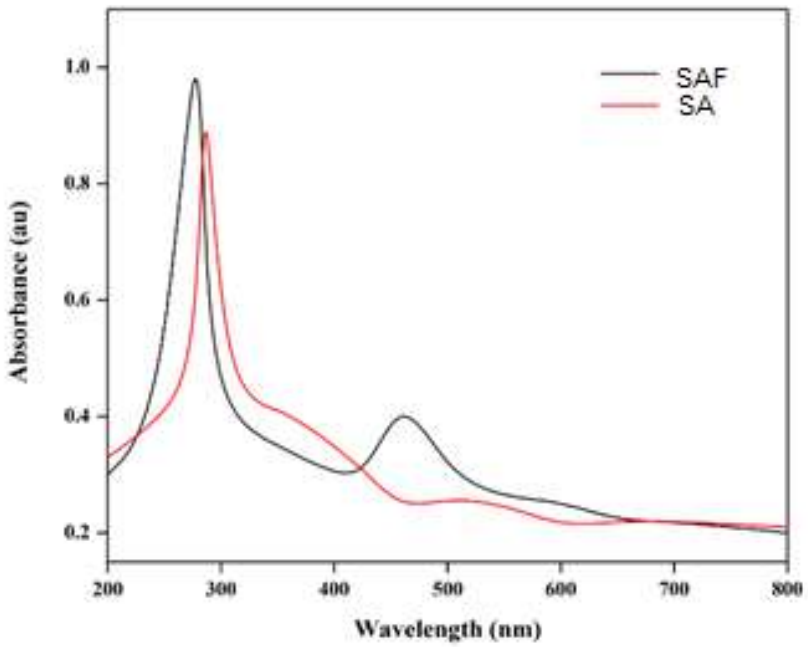


Fig. 26 UV-Vis spectra of syringic acid and syringic acid fraction

### 4.5.5 HPLC analysis of the syringic acid fraction

Further confirmation of the isolated fraction was preceded through HPLC analysis. The HPLC profile of the fraction 4 revealed characteristic peaks which matched well with the standard syringic acid. The retention time of fraction 4 was recorded at 2.088 min and 10.303 min which coincide well with the standard syringic acid peaks 2.097 min and 10.395 min thereby confirming the presence of syringic acid in the fraction (Fig.27a and 27b). Gini and Jothi (2018) analysed the presence of phenolic compounds such as ascorbic acid, quercetin, gallic acid, resorcinol, catechol, vanillin and benzoic acid through HPLC in *Salvinia molesta*. Butnaria and Coradini (2012) and Kannur and Khandelwal (2014) detected the presence of phenolic compounds and quercetin in the flower extract of *Calenula officinalis* and *Ficus carica* respectively.

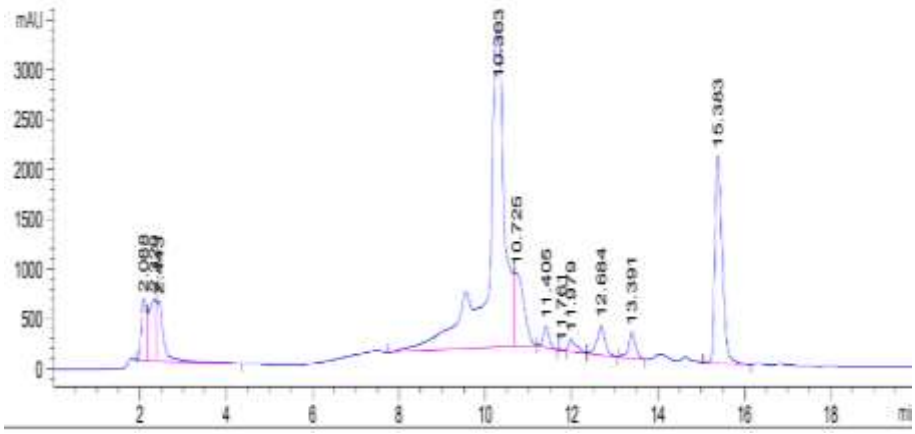


Fig. 27a HPLC profile of syringic acid fraction

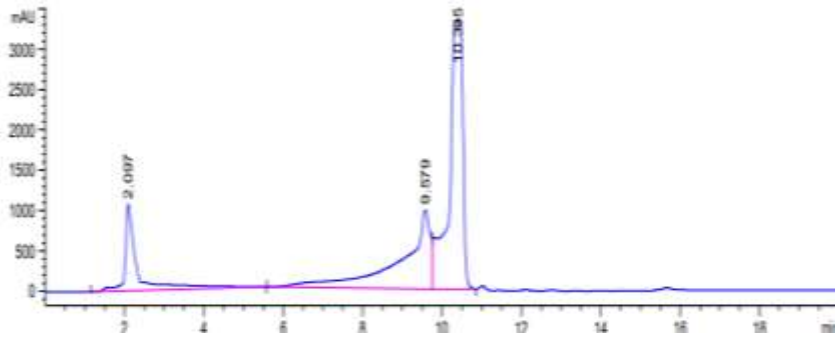


Fig. 27b HPLC profile of standard syringic acid

### 4.4.6 HPTLC analysis of the syringic acid fraction

The fraction 4 isolated from *P. amboinicus* was subjected to HPTLC analysis for the presence of syringic acid, a phenolic acid. The fraction 4 from *P. amboinicus* was run along with the commercially available standard syringic acid and its profile ($R_f$ values, height and areas of the peaks) was depicted in Table 11. The HPTLC profile of the isolated fraction 4 revealed $R_f$ value at 0.40 which corresponds well with the $R_f$ value of standard syringic acid ($R_f$ = 0.40) as can be observed from Table 11.

Hence the results implicits that the fraction 4 has prevailing amount of syringic acid along with the minor quantity of phenolic compounds. In the chromatogram, dark coloured bands were observed in the respective standard and sample tracks (Fig. 28).

Table. 11 HTPLC profile of standard syringic acid and isolated fraction 4

| Track | $R_f$ value | Height of the peak | Area of the peak |
|---|---|---|---|
| Std 1 | 0.42 | 682.3 | 21339.73 |
| 2 | 0.40 | 732.74 | 26950.01 |
| 3 | 0.39 | 722.70 | 27838.04 |
| 4 | 0.38 | 700.70 | 28729.37 |
| 5 | 0.38 | 713.22 | 32820.02 |
| Isolated fraction 4 | 0.40 | 733.67 | 33450.50 |

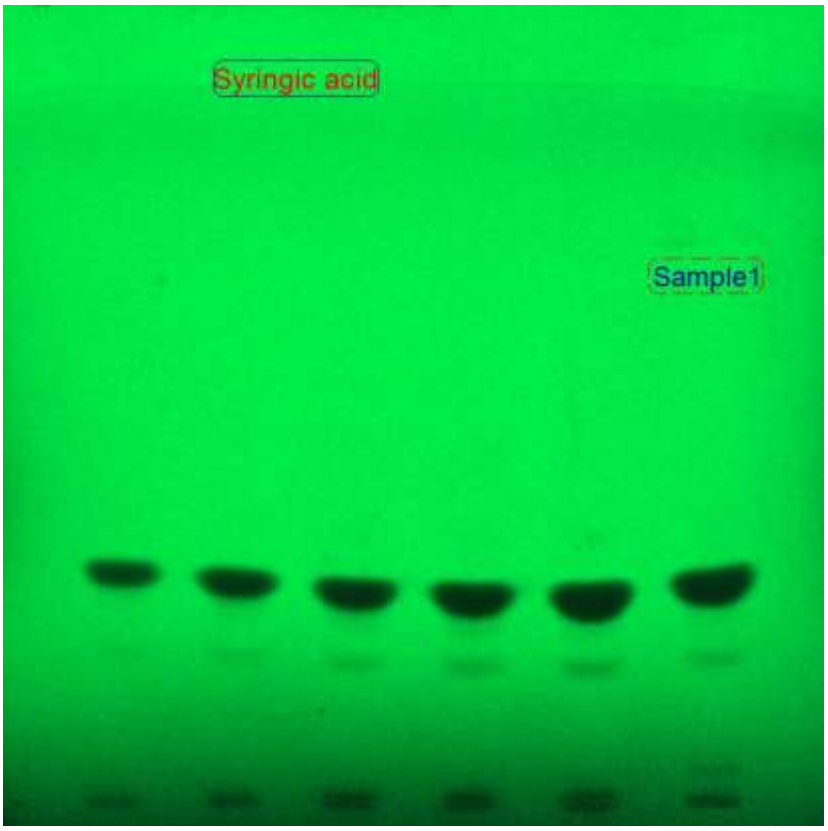


Fig. 28 HPTLC chromatogram of syringic acid and syringic acid fraction

The band in the sample track coincides with the standard thereby confirming the presence of syringic acid. The densitogram of the isolated fraction 4 matched well with the reference compound syringic acid and thereby confirms the presence of syringic acid in the fraction (Fig. 29a and 29b). Upadhye and Jain (2021) identified the phenolic acids namely gallic acid, vanillic acid and syringic acid in the seeds of *Phoenix dactylifera* seeds through HPTLC.

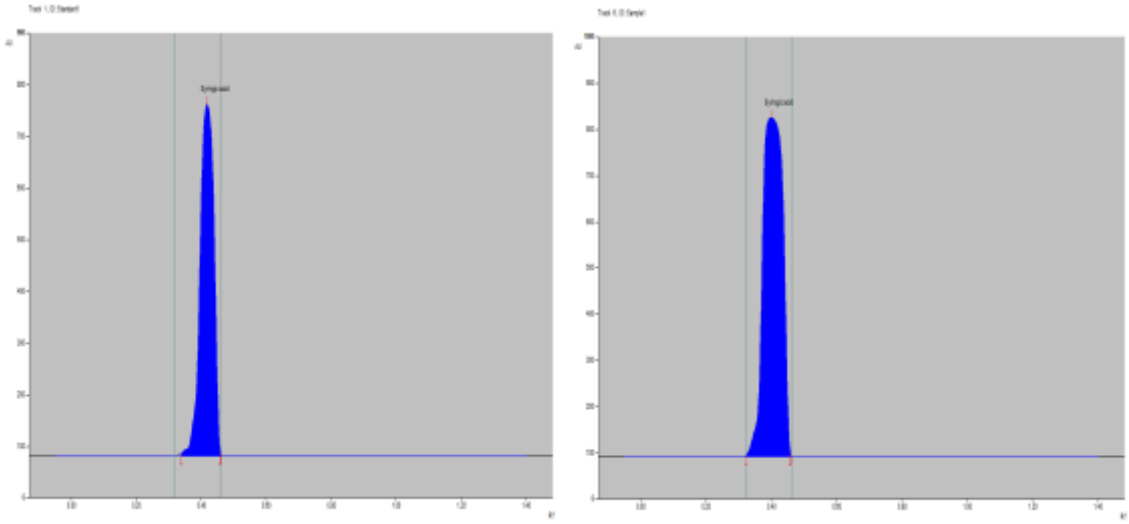

Fig. 29 HPTLC densitogram of syringic acid (a) and syringic acid fraction (b)

Thus the results of phase IV concludes the presence of phenolic acids in the leaf extract through FT-IR and NMR studies. Further elucidation confirms the presence of syringic acid in the fraction isolated from *Plectranthus amboinicus* through UV-Vis spectra, HPLC and HPTLC analyses. With this, the next phase was performed to analyze the impact of syringic acid fraction on the cytotoxic effect of A549 lung cancer cells through *in vitro* approach.

## PHASE V

### 4.5 CYTOTOXIC ACTIVITY OF SYRINGIC ACID FRACTION AGAINST A549 HUMAN LUNG CANCER CELLS - AN *IN VITRO* APPROACH

In recent past the research and development of anticancer agents from herbal products gains more attention, since they exhibit efficient and selective toxicity to tumor cells. It is evident from the results of Phase II and III that the

methanolic extract and the phytocompounds has the potent radical scavenging and anticancer activities. Further the presence of the compound of interest, syringic acid was confirmed through bioassay guided fraction was probed to investigate the cytotoxic and anticancer effect on A549 lung cancer cells and the results were compared with commercial syringic acid and the standard drug paclitaxel.

### 4.5.1 Cytotoxic activity of A549 cells using MTT dye reduction assay

The cytotoxic activity of SAF against the growth of A549 cells was evaluated by MTT assay. The viability of the SAF treated A549 cells was reduced based on dose-dependent manner and a half-maximum growth inhibitory concentration ($IC_{50}$) value of 29.82 µg/ml (Fig. 30) was observed after 24h of treatment.

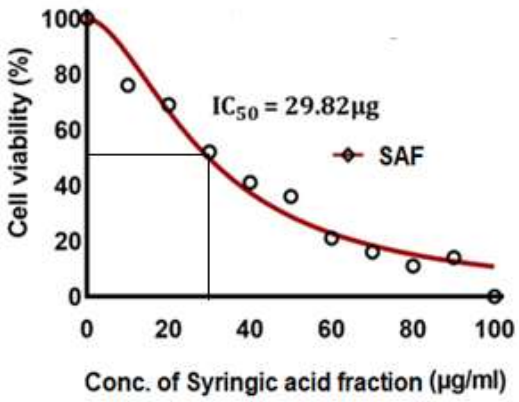


Fig. 30 Half-maximum growth inhibitory concentration ($IC_{50}$) of SAF through MTT assay

The morphological changes in the lung carcinoma cells were observed under the phase-contrast microscope. Compared with untreated lung cancer cells (Fig. 31a), SAF treated cells exhibited significant morphological transformations (Fig. 31d) as comparable with commercial syringic acid (Fig. 31c) and the standard drug paclitaxel (Fig. 31b) which reflected their cytotoxic potential. This in turn could be related to the formation of endogenous ROS, which can impede cell development.

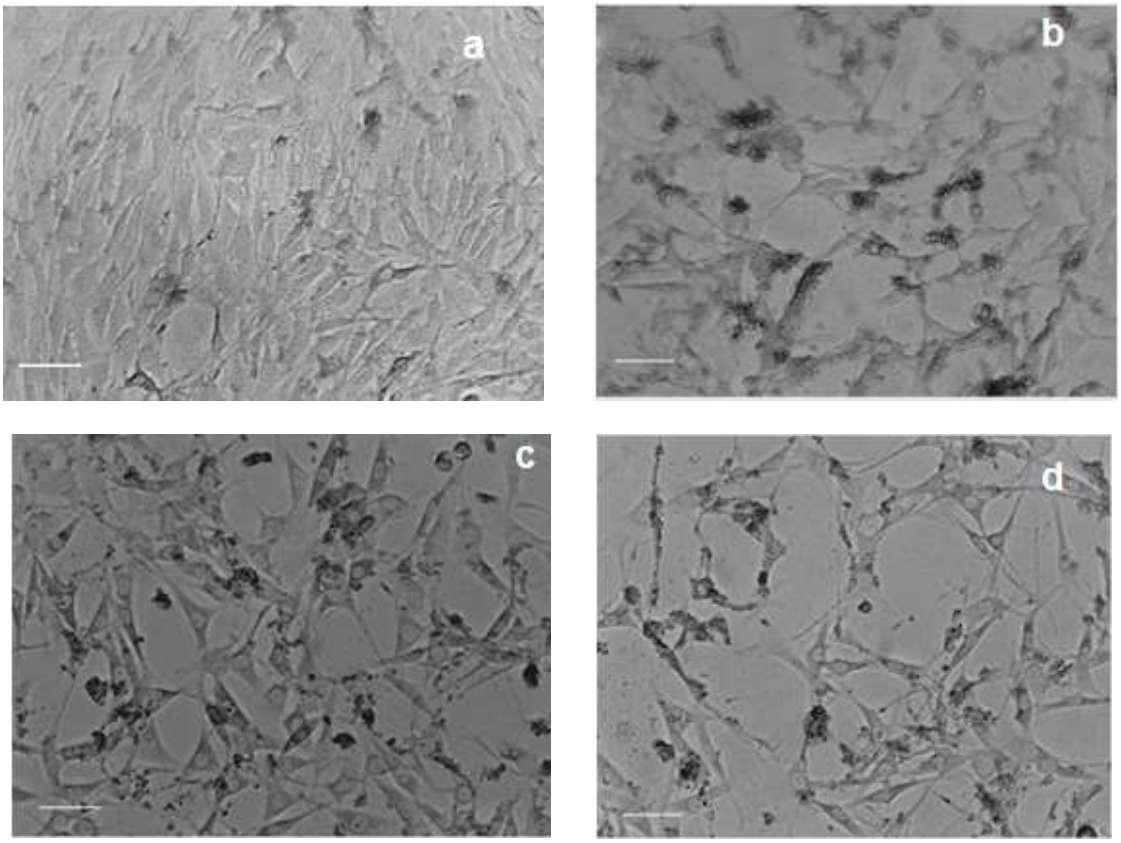


Fig. 31 (a-d) Morphological changes in A549 lung cancer cells
(a) Control (b) Paclitaxel (c) Syringic acid (d) Syringic acid fraction

In cancer cell lines, phenolic acids has been found to elicit cytotoxicity via ROS buildup and they are deliberated to exert antitumor properties by increasing the generation of free radicals and lipid peroxides, which can sequentially destroy proteins, enzymes, and ATP synthesis in cancer cells, eventually leading to apoptosis (Ma *et al.,* 2014). Presence of quercetin and coumarin in the leaf extract of *Cuphea ignea* was found to possess cytotoxic activity against non- small cell lung cancers (H460 and H23) as well as the human hepatocellular carcinoma cell line (Huh 7) (Gibellin *et al.*, 2011 and Moustafa *et al*., 2018). In line with the present study, Zheng *et al.* (2012) and Peng *et al.* (2015) observed the cytotoxicity effect against A549 cells which recorded significant $IC_{50}$ values when treated with tartariside B,C and D and p-coumaric acid respectively. The results of our study also coincides with the findings of previous investigation on the morphological changes and cytotoxicity effect of phenolic acids against carcinoma cells (Abaza *et al*., 2013; Myint *et al*., 2020; Chan *et al*., 2020).

Once the cytotoxicity of SAF was infered it is necessary to assess the mechanism of cell death induced by SAF. Hence, to define the contributory roles of SAF, the nuclear changes associated apoptosis were assessed in A549 lung cancer cells through various staining techniques, and compared with commercial syringic acid and standard drug paclitaxel.

### 4.5.2. Nuclear change analyses by AO/EtBr, DAPI and PI staining

The major hallmark in cancer studies is the disruption of apoptotic pathway. The endogenous nucleases get activated and cleave the DNA into oligonucleosomal fragments during apoptotic cell death. This lead to the fragmentation of nucleus into apoptotic bodies which is viewed as dense and crescent shaped chromatin aggregates (Wong, 2011). The nuclear changes and apoptotic body formation of SAF on A549 cells were determined by acridine orange/ethidium bromide (AO/EtBr) staining. The AO stains both the survived and dead cells and produce green fluorescence (Fig. 32a), whereas EtBr stains the membrane damaged cells and generate red fluorescence.

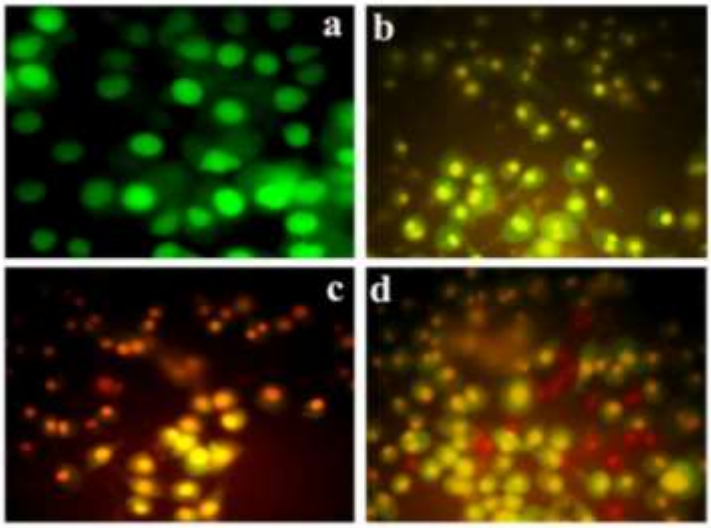


Fig. 32 (a-d) Apoptotic analysis using AO / EtBr staining in A549 cells

(a) Control (b) Syringic acid fraction (c) Syringic acid (d) Paclitaxel

As a result of chromatin condensation and nuclear fragmentation, early apoptotic cells stained green and have vivid green spots in the nucleus. Ethidium bromide will be absorbed by late apoptotic cells, causing them to colour orange

(Liegler *et al*., 1995). The induction of apoptosis and nuclear condensation effect attributable to the action of SAF, SA, and paclitaxel was related to the induction of apoptosis and nuclear condensation as depicted in Fig. 32(b-d). The dead cells which stained orange, suggest condensed, cell shrinkage, membrane blebbing, and nuclear fragmentation (Erenpreisa *et al.,* 1997 and Kumar *et al*., 2014).

The nuclear DNA morphology of A549 cells treated with SAF, syringic acid and paclitaxel was determined by DAPI staining. The immunofluorescent test was used to determine the potential nuclear modifications such as genomic DNA fragmentation (Patil *et al*., 2018). Due to the presence of intact nucleus, the untreated cells display a weak excitation of the fluorescent light (Fig. 33a), whereas the SAF, SA, and paclitaxel treated cells (Fig. 33b -33d) revealed brilliant bright fetches, indicating the formation of condensed chromatins and nuclear fragmentations. Thus the results revealed that SAF treated A549 cells indicated the formation of apoptotic bodies which lead to cell death as comparable with syringic acid and paclitaxel.

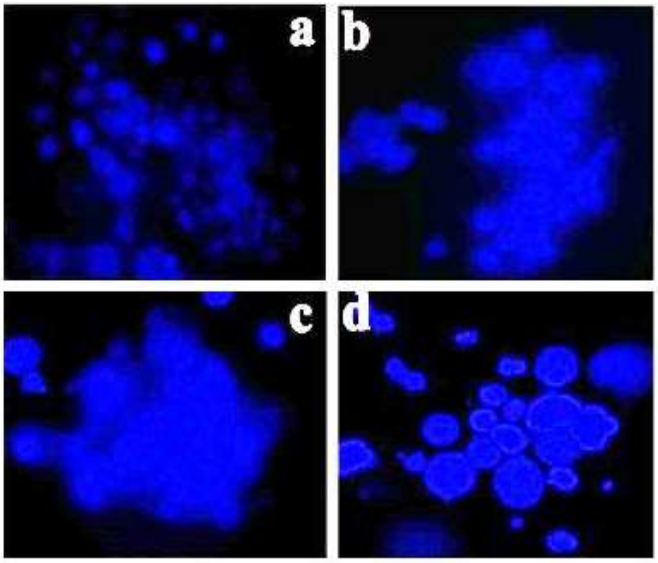


Fig. 33 (a-d) Nuclear fragmentation analysis using DAPI staining in A549 cells
(a) Control (b) Paclitaxel (c) Syringic acid (d) Syringic acid fraction

Propidium iodide (PI), a membrane-impermeant dye is widely used for cell identification has increasing permeability to cells undergoing apoptosis, even

though it is a huge molecule that can enter live and active cells. Hence, PI staining is determined as an index of the level of apoptosis in cells (England *et al*., 2004). The control cells did not show any nuclear fracture (Fig. 34a), whereas more apoptotic cells were seen in SAF as comparable with syringic acid and paclitaxel treated cells (Fig. 34b-d) due to the conformation of higher genomic DNA fragmentation. The phenolic compounds react with cancer cells and cause membrane damage, genomic DNA damage, cell shrinkage and under morphological changes in cells thereby leading to cell death (Niyonizigiye *et al*., 2020 and Patra *et al*., 2020).

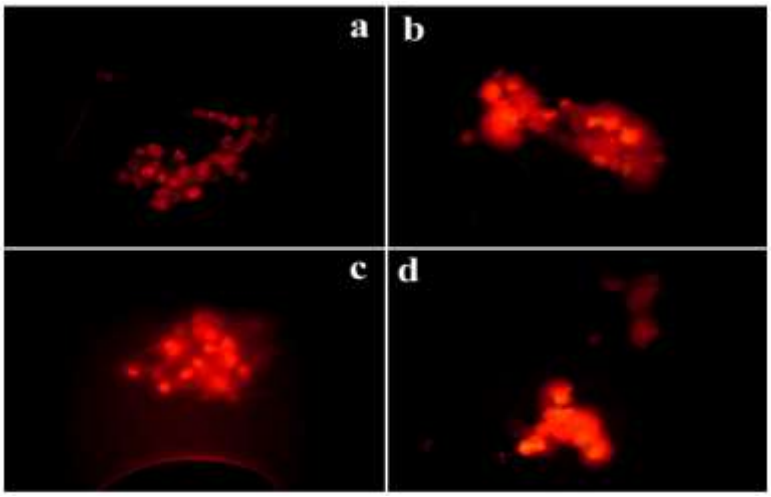


Fig. 34(a-d) Propidium iodide staining showing nuclear morphological differences

(a) Control (b) Paclitaxel (c) Syringic acid (d) Syringic acid fraction

The results of the staining techniques revealed that syringic acid fraction induced apoptotic cell death in A549 cell lines as it exhibited nuclear changes, the characteristic feature of apoptosis. Syringic acid fraction can be used as a potent therapeutic agent since it clearly expressed its action against the lung cancer cells, as comparable with commercial syringic acid and he standard drug paclitaxel.

### 4.5.3 Detection of apoptotic events in A549 cells

An apoptotic analysis using flow cytometry was used to investigate the approach by which the syringic acid fraction has a deleterious effect on lung cancer cells. The scatter plot of the flow cytometric analysis present the

consequent distribution of cells, which are defined as follows, live cells in the lower left quadrant (Q1), the early apoptotic cells in the lower right quadrant (Q2), the late apoptotic cells in the upper right quadrant (Q3) and the necrotic cells are in the upper left quadrant (Q4) (Ramya *et al.,* 2021). The movement of phosphatidyl serine from the inner to outer surface of the plasma membrane of cells is a crucial aspect of apoptosis. The phospholipid constituent is usually situated on the membrane of live cells. When a cell undergoes an apoptotic process, phosphatidyl serine is no longer restricted to the cytosol, but is also exposed on the cell surface. As a result, phosphatidyl serine translocation is a biochemical marker of apoptosis, instigates DNA fragmentation which is the hallmark of apoptosis. The results indicate that A549 cells treated with SAF revealed 52.81% of early apoptotic cells and 31.75% of late apoptotic cells (Fig. 35d), whereas syringic acid and paclitaxcel, the standard drug used for the treatment of lung cancer could induce apoptosis readily as evidenced by the presence of more cells in the late apoptotic phase (Fig. 35a-35c).

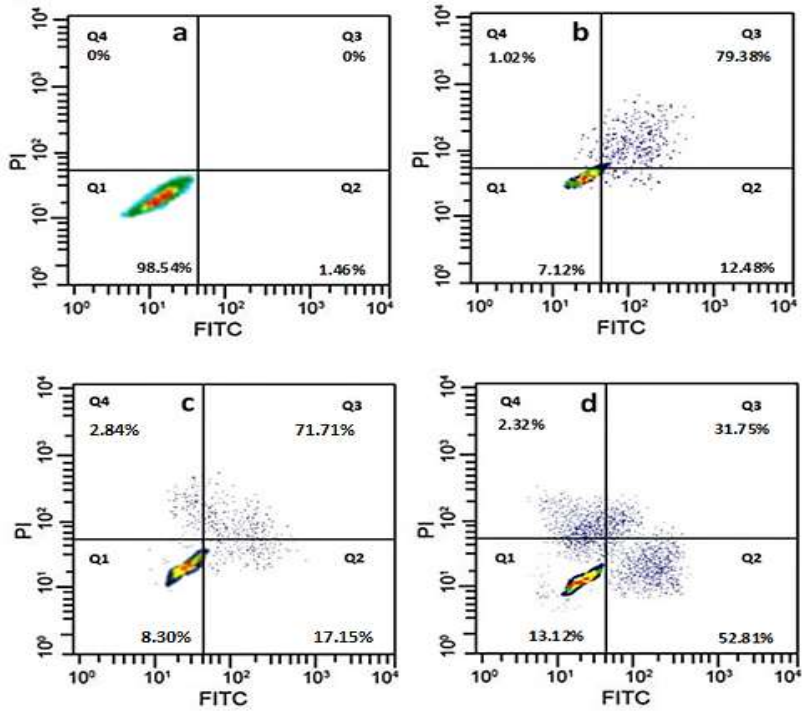


Fig. 35 (a-d) Annexin V/PI assay depicting the apoptosis-inducing effect on A549 cells

(a) Control (b) Paclitaxel (c) Syringic acid (d) Syringic acid fraction

A significant increase in the apoptotic cells from early to late apoptotic stage was recorded in cell treated with *Datura innoxia* extract (5µg/ml). In the same manner, an increase in apoptotic cells was recorded for both stages after treatment with 10µg/ml of *Datura innoxia* extract. This strong shift in early and late apoptotic cell populations and absence of necrotic cells emphasizes that *Datura innoxia* extract exerted apoptosis cell death mode (Al-Zharani *et al*., 2021).

The ability of methanolic leaf extracts of *Holarrhena floribunda* to induce apoptosis in breast (MCF-7), colorectal (HT-29) and cervical (HeLa) cancer cells was investigated and the results revealed that HT-29 cells underwent early apoptosis, while HeLa cells underwent late apoptosis, yet MCF-7 cells underwent necrosis after 48h (Badmus *et al*., 2015).

The results of the present study revealed that the SAF was able to induce cell death mediated by apoptosis in the A549 cell line at early apoptotic stage and further to late apoptosis as comparable with syringic acid and the drug, paclitaxel which mediated apoptosis at late apoptotic stage which was confirmed by Annexin V / FITC staining.

### 4.5.4. Determination of cell cycle analysis by Annexin V / FTIC staining

Cell cycle is a series of events that occur in a cell that lead to its division and DNA replication, resulting in the formation of two daughter cells. Inhibition of cell growth and activation of apoptosis process would occur if the cancer cell cycle was disrupted. Hence, cell cycle analysis is considered essential in the diagnosis and treatment of diseases. It is used to recognize the DNA profile and the distribution of cell populace in the G0/G1, S and G2/M phases which was determined by the evaluation of DNA contents based on the fluorescence intensity. Cell death is arbitrated by cell cycle arrest which is witnessed using flow cytometry to confirm at which phase the A549 cell lines got arrested when they were treated with SAF, SA and PA. It is evident from Fig. 36a that the untreated A549 cells were uniformly scattered in all the phases namely, G0-G1, S and G2/M phase and regular events of cell cycle was illustrious in this group. Flow cytometry analysis of A549 cells treated with SAF revealed an increase in the percentage of cells in G0/G1 phase with a concurrent decrease or transitional arrest in S-phase,

as compared to commercial syringic acid and the reference drug, paclitaxel. This signifies that the SAF inhibited the proliferation of A549 lung cancer cells through arresting G0/G1 cell cycle phase progression. The cell cycle arrest in G2/M phase can reduce the growth and trigger apoptosis by inhibiting the separation of damaged chromosomes during mitosis [Fig. 36(b-d)]. Altogether it was observed that SAF potently induced cell growth inhibition, G2/M cell cycle arrest, and apoptosis in lung cancer cells as comparable with syringic acid and paclitaxel.

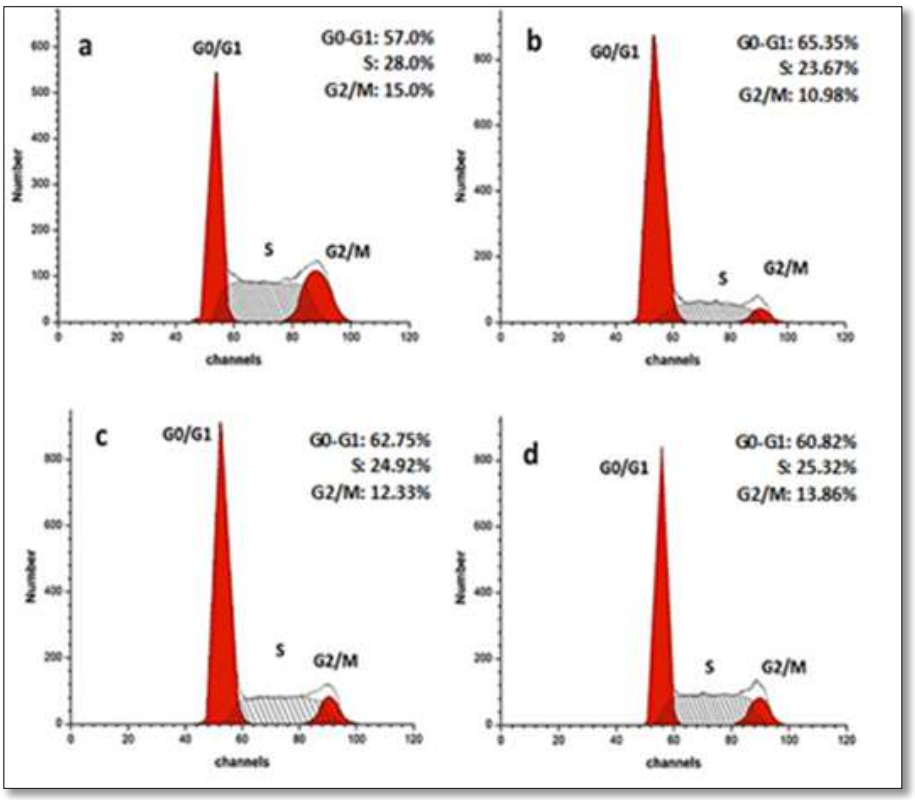


Fig. 36 (a-d) Cell cycle arrest on A549 cells (a) Control (b) Paclitaxel (c) Syringic acid (d) Syringic acid fraction

When cell cycle progression is arrested or delayed by a drug/compound, it allows time for DNA repair, or when damage is permanent, it causes cellular senescence, which is regulated by signalling pathways known as cell cycle check points and stops cell growth indefinitely (Lukas *et al.,* 2004). They may stifle tumorigenesis mainly through probing the mitotic spindle dynamics and trigger the mitotic checkpoint, thus inducing an unmitigated G2/M arrest (Zhu *et al.,* 2018). Similar results were acquired with MCF-7 cells, which arrested the G2/M phase

and induced apoptotic cell death (Wang *et al*., 2020 and Tripathi *et al*., 2020). Li *et al*. (2018) and Clemento-Soto *et al*. (2019) reported that Biochanin A induced cell cycle arrest significantly at S phase in lung cancer cells (A549 and 95D) and querticin induced G2 phase cell cycle arrest and apoptosis in both human cervical cancer HeLa and SiHa cells, accompanied by an raise of p53 and its nuclear signal respectively. Exposure of myriceitin and methyl eugenol combination enhances blocked cell cycle progression at G0/G1 check point in HeLa cervical cancer cells (Yi *et al*., 2015). Thus, the results of the flow cytometric studies stated that syringic acid induced cell death by apoptosis in A549 lung cancer cells.

The findings of the present study are consistent with the reports of Aliyu *et al.,* (2013) who observed the induction of cytotoxicity on human lung cancer NCI-H460, human A375 and murine B16-F1 melanoma cells by acacia honey. It blocked the progression of cell cycle in G0/G1 phase and down regulated the Bcl2, P5 genes and G2/M phase. Chen *et al*. (2015) also observed the G0/G1 and G2/M arrest on human liver cancer cell smmc-7721, stomach cancer cell BGC-823 and breast cancer MCF-7 cells using *Cordyceps militaris* polysaccharides.

Similarly, the G2/M arrest is associated with DNA damage and affords the cells, to get repaired in tissues before entering into mitosis, thereby inhibits the persistence of genomic mutations (Stark and Taylor, 2004). The human breast MCF-7 and A549 lung cancer cell proliferation in G2/M phase were inhibited by *Acacia nilotica* extract and γ-sitosterol (Sundarraj *et al*., 2012), MCF-7 cells by *Mangifera pajang* kernel (Bakar *et al*., 2010) and brain cancer cells by plumbagin (Khaw *et al*., 2015). The ethanolic extract of *Clitocybe alexandri* and Capilliposide from *Lysimachia capillipes* Hemsl arrested the growth of NCI-H460 and H460 lung cancer cell lines (Vaz *et al*., 2012 and Fei *et al*., 2014).

Thus, the results of cell cycle analysis support the previous findings, indicating that SAF induced cell growth arrest in the S and G2/M phases in A549 cell lines and was found to be effective as comparable with the chemotherapeutic drug, paclitaxel and commercial syringic acid.

### 4.5.5. Regulation of protein and gene expression by Western Blotting and RT - PCR

The study was further designed to determine the mechanism behind the apoptotic induction by assessing the changes in the level of expression of apoptosis -related protein / gene expression which is crucial for lung cancer treatment. Using Western blotting and RT-PCR techniques, the transformation or changes in the expression level of apoptosis related genes namely p53, caspase 3, cytochrome C (apoptotic protein) and Bcl-2 (antiapoptotic protein) were treated with $IC_{50}$ concentration of SAF and compared with the positive controls such as syringic and paclitaxel to investigate the mechanism of action. In both experiments, beta actin was used as a housekeeping control. Fig. 37a and Fig. 38a revealed remarkable upregulation in the expression of caspase, p53 and C while a notable down-regulation was observed in the anti-apoptotic protein, Bcl - 2. Fig. 37b and Fig. 38b represents the relative protein and gene expression of fold changes in Western blot and RT-PCR respectively.

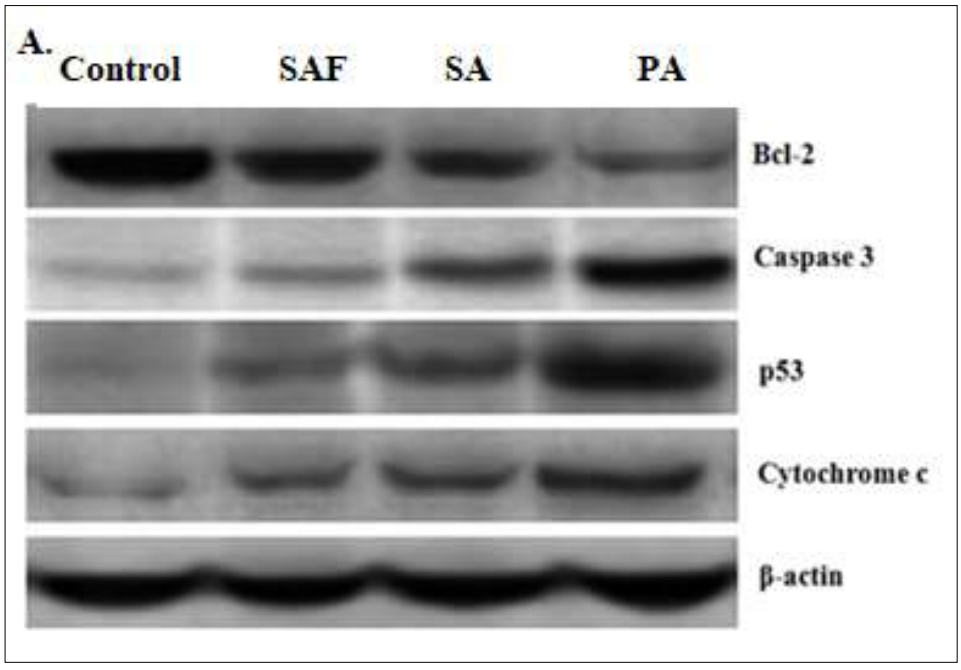


Fig. 37a Effect of SAF, syringic acid and paclitaxel on protein expression using Western blotting

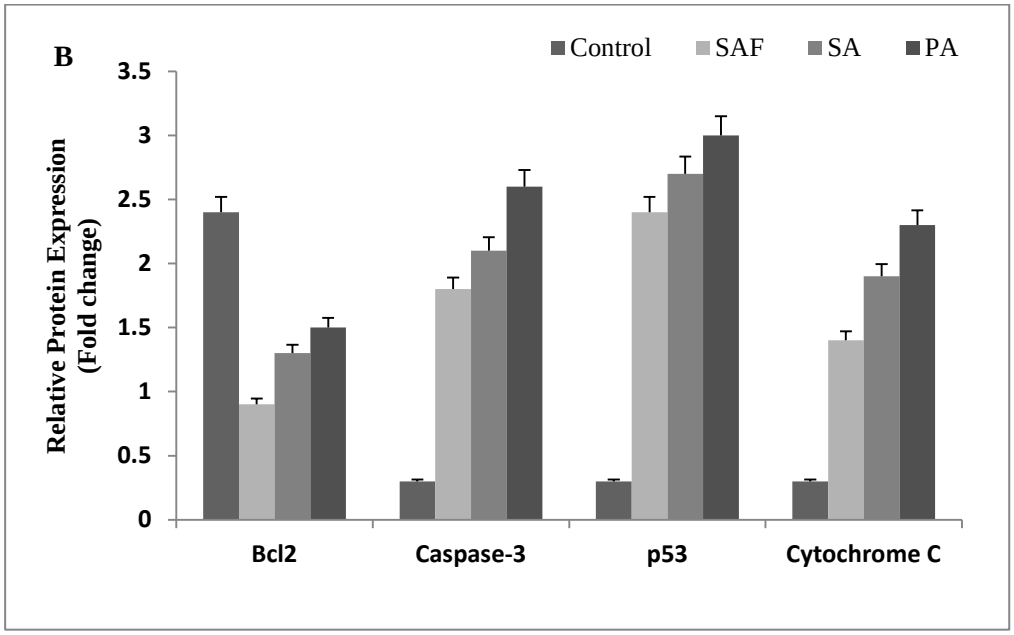


Fig. 37b Densitometry representing the relative protein expression in Western Blot

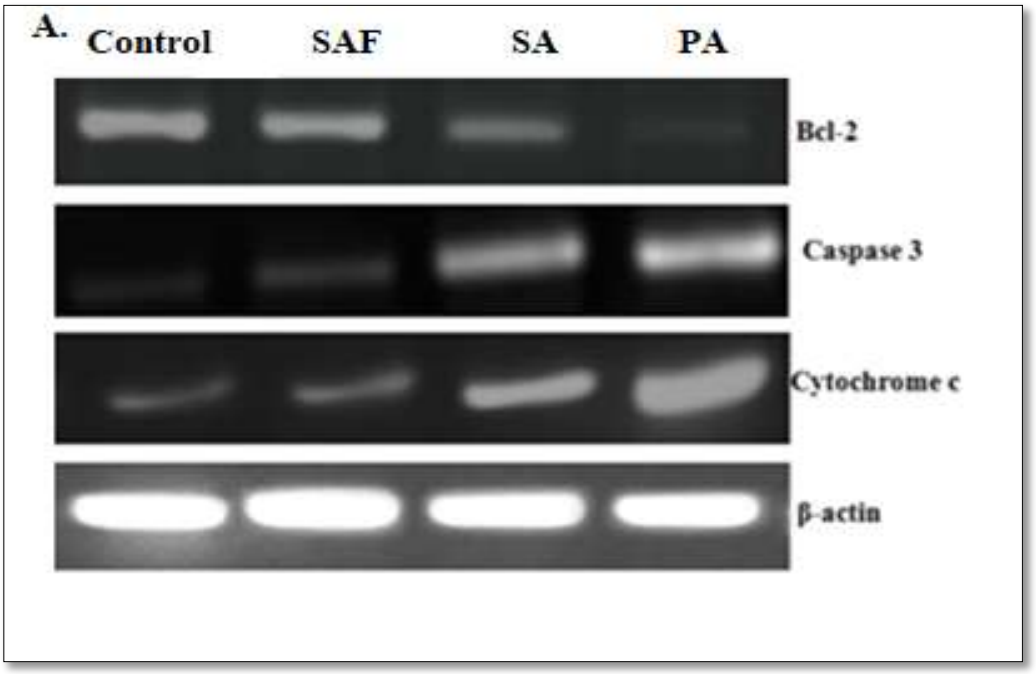


Fig. 38a Effect of SAF, SAF, syringic acid and paclitaxel on gene expression using RT-PCR

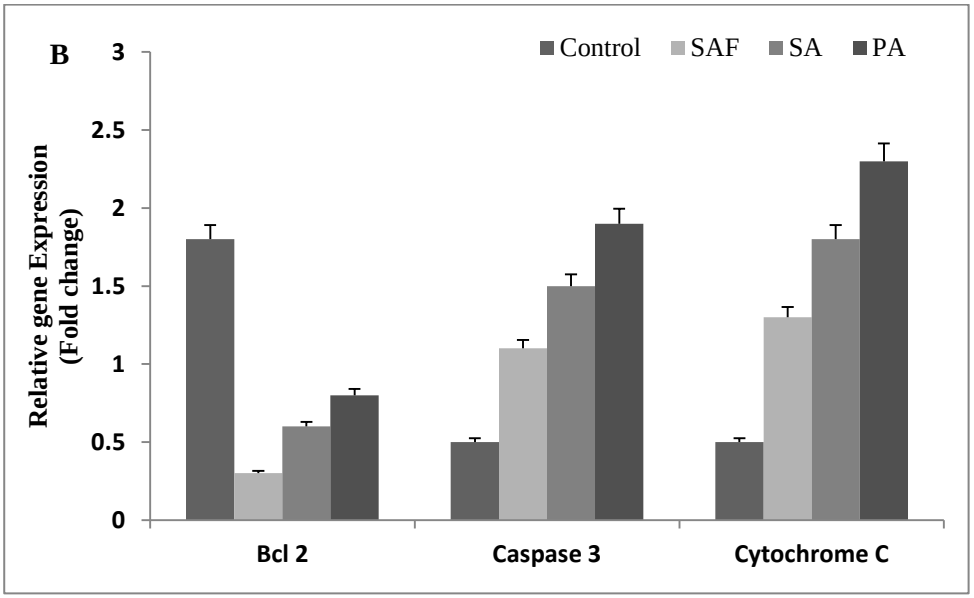


Fig. 38b Densitometry representing relative gene expression in RT-PCR

Notably, the results of the present study are consistent with the path in which the depletion or downregulation of anti-apoptotic proteins causes mitotic distress, DNA damage and finally cell apoptosis. The decreased level of Bcl-2, illustrated that SAF frequently arbitrated the innate apoptotic process by stifling the antiapoptotic expression. Previous report by Oren and Rotter (1999) confirmed that tumor suppressor protein p53 plays a central role in determining the oncogenic transformation from cancer treatment and more than 50% of the cancer related to human beings occurs due to the defects in p53. Also, to execute apoptosis in cancer cells, the over expression of p53 is required. Earlier research findings strongly denoted the increase in caspase-3 and low level of Bcl-2 stimulated apoptosis on A549 cells which supported the findings of the present study (Chan *et al*., 2020).

Zhang *et al*. (2018) also reported that Bax plays a pivotal role the inhibition of Bcl-2 and it's over expression suppresses the cytochrome C release from mitochondria to cytoplasm and obstructs the initiation of caspase in the mitochondrial mediated neutral apoptotic pathway. Cao *et al*. (2018) also observed upregulation of apoptotic related genes such as caspase 3, caspase 6 and Apaf-1 in HCT116 and SW480 colon cancer cells. Cicin *et al*. (2015) reported

that hesperidin inhibited the proliferation and induction of apoptosis via loss in mitochondrial membrane potential, activation of caspase 3 and affects fibroblast growth factor and NF – KB signal transduction in A549 and NCI358 cells.

Gheena and Ezhilarasan (2019) reported that the apoptotic markers such as caspases 3 and 9, cytochrome C, Apaf-1, Bax, and p53 gene expressions were increased significantly with SA treatment demonstrating the possibility of apoptosis induction in HepG2 cells and also caused significant downregulation of Bcl-2 gene expression. Chia *et al*. (2010) also reported that phenolic acids induces mitochondrial membrane depolarization and release second mitochondria-derived activator of caspase (SMAC) protein from mitochondria into the cytosol to control cancer and thereby reflects their anticarcinogenic potential.

### 4.5.6. Mechanism of SAF in the activation of apoptosis

To explore the mechanism implicated in apoptosis stimulation, the molecular mechanism was assessed (Fig. 39). During tumorigenesis, considerable loss or inactivation of caspases leads to impair apoptosis induction, causing a remarkable imbalance in the growth dynamics, eventually ensuing in the abnormal growth of human cancers (Patil *et al*., 2018). Programmed cell death or apoptosis is a pivotal process that regulates tissue homeostasis and stress response. Apoptotic induction occurs either through extrinsic pathway / death receptor which is activated by exogenous death – inducing ligands and intrinsic/ mitochondrial pathway which is induced by stress conditions. Studies conducted by various researchers revealed that activation of apoptosis is a crucial step in initiation and progression of cancer. Generation of Reactive Oxygen Species in intracellular signalling and metabolic pathways is inevitable since it leads to oxidative stress causing cell damage which subsequently induces intracellular oxidation of molecules, mitochondrial membrane potential disruption and finally results in apoptosis. During this process the antiapoptotic protein/gene Bcl-2, prevent apoptosis either by sequestering the activity of caspases or by inhibiting the release of mitochondrial apoptogenic factors such as cytochrome C into the cytosol. Results of the present study demonstrated that SAF downregulated the level of antiapoptotic protein/gene Bcl-2 and upregulated the proapoptotic

protein/gene. The overexpression of BAX may results in the mitochondrial translocation, altered protein interaction in mitochondrial membrane which thereby opens the transition pores and disrupts the membrane potential. Furthermore, after being triggered by a number of apoptosis inducing factors, p53, which protects genomic stability, activates checkpoints and tumorigenesis, and liberates cytochrome C from mitochondria to cytosol, resulting in the formation of apoptosome. This creates a platform for the effective processing and activation of caspase 9, which then cleaves effector caspases like caspase 3 and 7, causing apoptosis in A549 lung cancer cells.

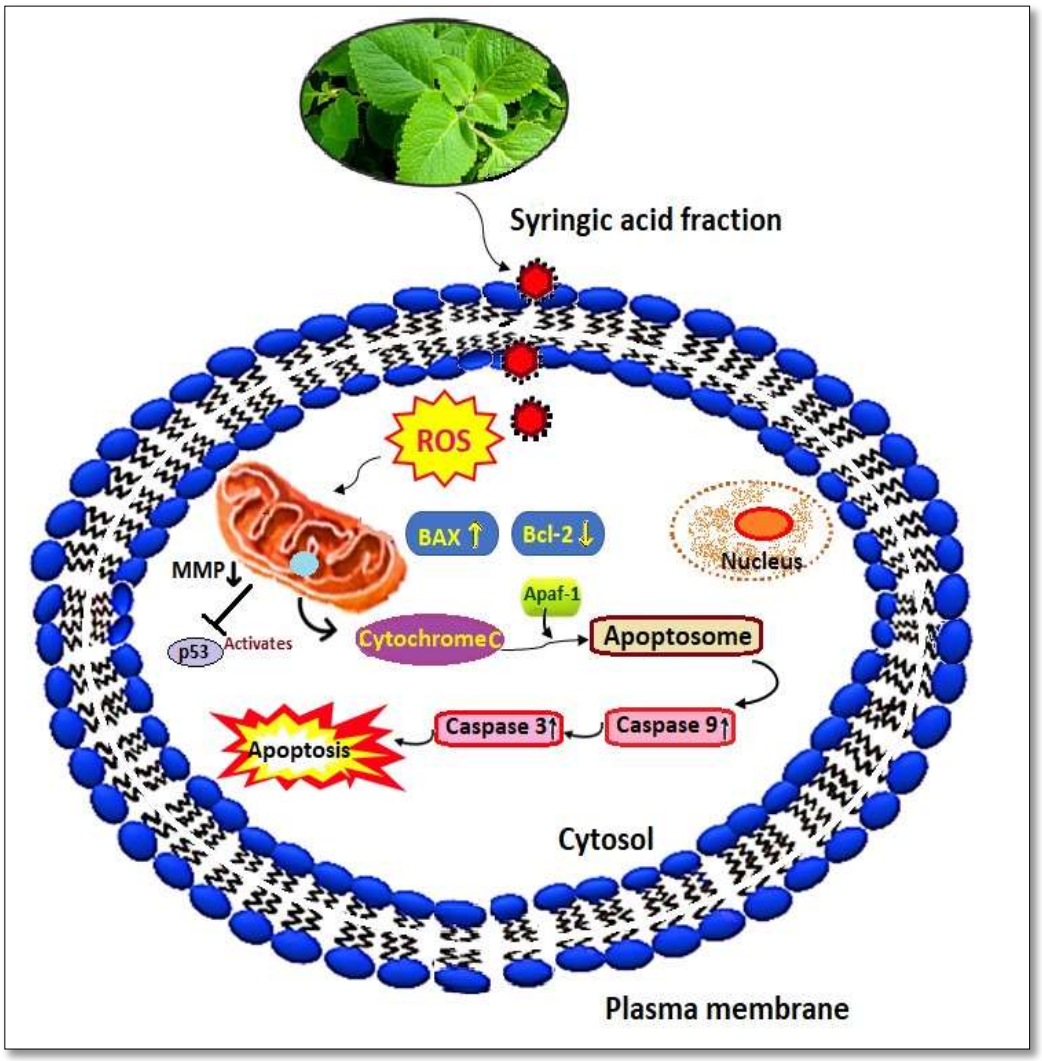


Fig. 39 Diagrammatic illustration of syringic acid fraction inducing apoptosis in A549 cells

Thus the findings of the present study confirmed that syringic acid fraction could result in the up regulation of p53, caspase 3, cytochrome C (apoptotic proteins) and down regulation of Bcl-2 (antiapoptotic protein) proving that SAF could cause the death of A549 lung cancerous cells. The altered expression was observed in the presence of SAF occurred via intrinsic pathway mediated by disruption of mitochondrial membrane. It can be inferred that this strategy could be adopted for the development of drugs using SAF for the studies that could substantiate the drug discovery process.

To summarize the results of phase V, the treatment with SAF resulted in cytotoxicity against A549 lung cancer cell lines. The results of staining techniques, Annexin V / FTIC-PI assay, cells cycle arrest and protein / gene expression showed that SAF have potential toxicity towards cancer cells. SAF also exhibited differential effect when tested for its capability to influence apoptotic / antiapoptotic gene expression in A549 lung cancer cell lines. Thus, the above results confirm that syringic acid fraction can be used as a potent therapeutic agent since it clearly expressed its action against the lung cancer cells, as comparable with commercial syringic acid and he standard drug paclitaxel.

## PHASE VI

## 4.6 ANTICANCER ACTIVITY OF SYRINGIC ACID FRACTION IN BENZO(A)PYRENE INDUCED EXPERIMENTAL MICE – AN *IN VIVO* APPROACH

Following the studies of *in vitro* cytotoxic activity of syringic acid fraction (SAF), the same was tested using Swiss Albino mice as experimented animal. The *in vivo* study was carried out to confirm the role played or evolved by the drug / compound / extract on the physiological systems which influence the biological response (Lipinski and Hoppins, 2004).

### 4.6.1 Acute toxicity

Acute toxicity is defined as the adverse effect that occurs either immediately or at a short time interval after administration of a drug/ compound within 24 hours. Studies on acute toxicity tend to establish the dose-dependent

adverse effect, which is important in its assessment including mortality. The assessment of the lethal dose ($LD_{50}$) (the dose that kills 50% of test animals population) has now been used as a major parameter in measuring acute toxicity and also as an initial procedure for general screening of chemical and pharmacological agents for toxicity. Apart from mortality, other biological effects and the time of onset, duration and degree of recovery on survived animals, are also important in acute toxicity evaluation. Hence acute toxicity assessment of pharmacological compound/ drug is a very important procedure to be carried-out before they are allowed to enter the market for sale (Akhila *et al*., 2007). The results of acute toxicity revealed that there was no lethal activity or death in mice treated with syrinigic acid at the dosage of 25 to 300 mg/kg. Clinical manifestations like tremors, pilo erection and abdominal breathing were observed at the oral dosage above 250 mg/kg. Based on these $LD_{50}$ (Dixons likelihood) values, $1/5^{th}$ of the dose (50mg/kg) and $1/10^{th}$ of the dose (25 mg/kg) of SAF was selected as lower and higher dose for further studies (Table 12).

Table 12. Effect of acute oral administration of syringic acid fraction on Swiss Albino mice

| Dose (mg/kg) | Latency | Symptoms |
|---|---|---|
| 0 | - | None |
| 50 | - | None |
| 100 | - | None |
| 150 | - | None |
| 200 | - | None |
| 250 | - | None |
| 300 | - | Tremors, pilo erection, abdominal breathing |

### 4.6.2. Effect of syringic acid fraction on tumor growth factors

#### 4.6.2.1 Mean survival time

The mean survival time for B(a)P induced Swiss albino mice was 11 days. When the mice were treated with SAF the mean survival time was increased (15 days) as comparable with those augmented with paclitaxel (16.66 days) and commercial syringic acid (15.33 days). The mean survival time of mice treated with syringic acid alone was reliable with normal control as depicted in (Fig. 40). The results fall in line with Kumar *et al.* (2011) who also described the increase in mean survival time of EAC and DLA tumor induced Swiss albino mice treated with higher dose of methanolic extract of *Indigofera cassiodies* as compared with the tumor control.

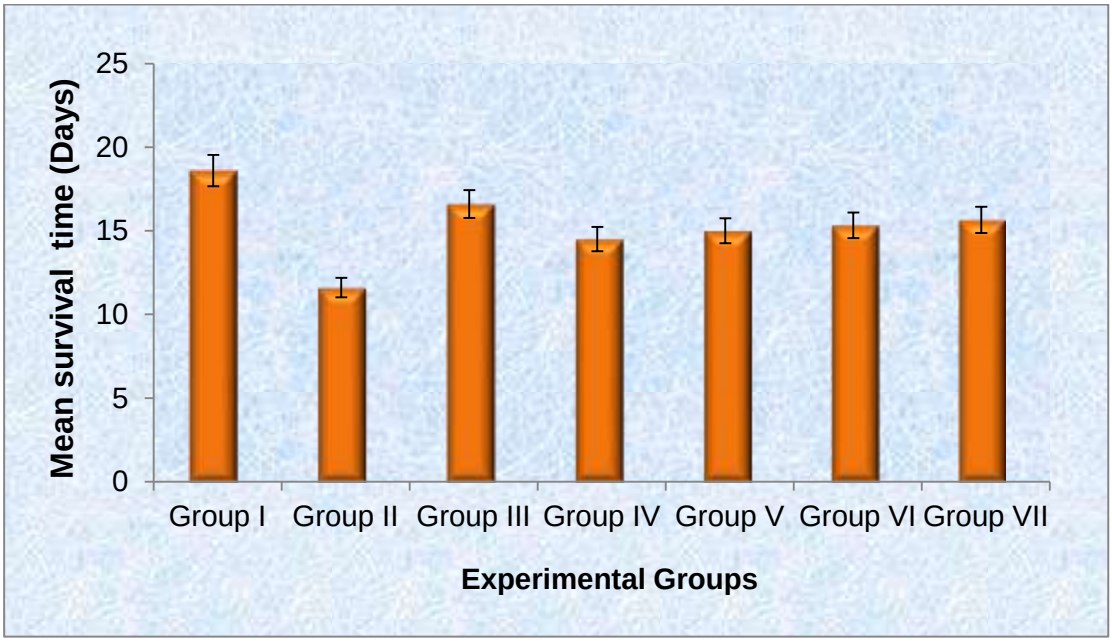


Fig. 40 Mean survival time of the experimental mice under various treatments

Thus the results confirmed that the mice treated with SAF has significant antitumor activity as it increases the survival days of B(a)P induced mice as comparable with standard drug paclitaxel and syringic acid.

#### 4.6.2.2 Increased life span

The increase in life span is one of the most vital criteria for the foremost assessment of a compound's antitumor activity. Andreani *et al.* (1983) reported

that a compound is said to have significant antitumor activity if it increases the life span by 25%. While evaluating antitumor activity, the results of the survival analysis should be taken into account. The results of the present study illustrated that SAF (25 and 50mg/kg) exhibited significant antitumor activity (25% and 29%) against B(a)P induced lung cancer mice was compared with the standard drug paclitaxel (43%) and syringic acid (32%) (Table 13). Thummar *et al*. (2015) and Saroja and Annapoorni (2011) reported the antitumor activity of cleistanthin B (50mg/kg) and *Terminalia catappa* which increased the life span by 65% and 90% against Swiss albino mice induced with DAL and ELA.

Table 13. Increased life span of the experimental mice under various treatments

| Groups | Treatment | Increased Life Span (%) |
|---|---|---|
| I | Control | 0 |
| II | B(a)P (50 mg/kg) | 0 |
| III | B(a)P + Paclitaxel (5mg/kg) | 43 |
| IV | B(a)P + Syringic acid fraction (25 mg/kg) | 25 |
| V | B(a)P + Syringic acid fraction (50 mg/kg) | 29 |
| VI | B(a)P + Syringic acid (25mg/kg) | 32 |
| VII | Syringic acid (25mg/kg) | 35 |

Thus the results revealed that SAF has a significant antitumor activity as it increases the life span of B(a)P induced mice to more than 25% thereby suggesting its therapeutic potential in curing cancer.

### 4.6.2.3 Analysis of body weight

The effect of syringic acid fraction on the body weight of the experimental mice was measured on initial and final day of the experimental period and the results were depicted in Fig 41. Mice treated with B(a)P (Group II) exhibited

significant reduction in the body weight as compared with normal control mice. Oral administration of mice with syringic acid fraction at the dose of 25mg/kg (Group IV) and 50mg/kg body weight (Group V) showed a significant increase in their body weight as the experimental period increases and the results are comparable with Group III animals. Mice administered with syringic acid alone (Group VII) showed significant body weight as that of control mice (Group I).

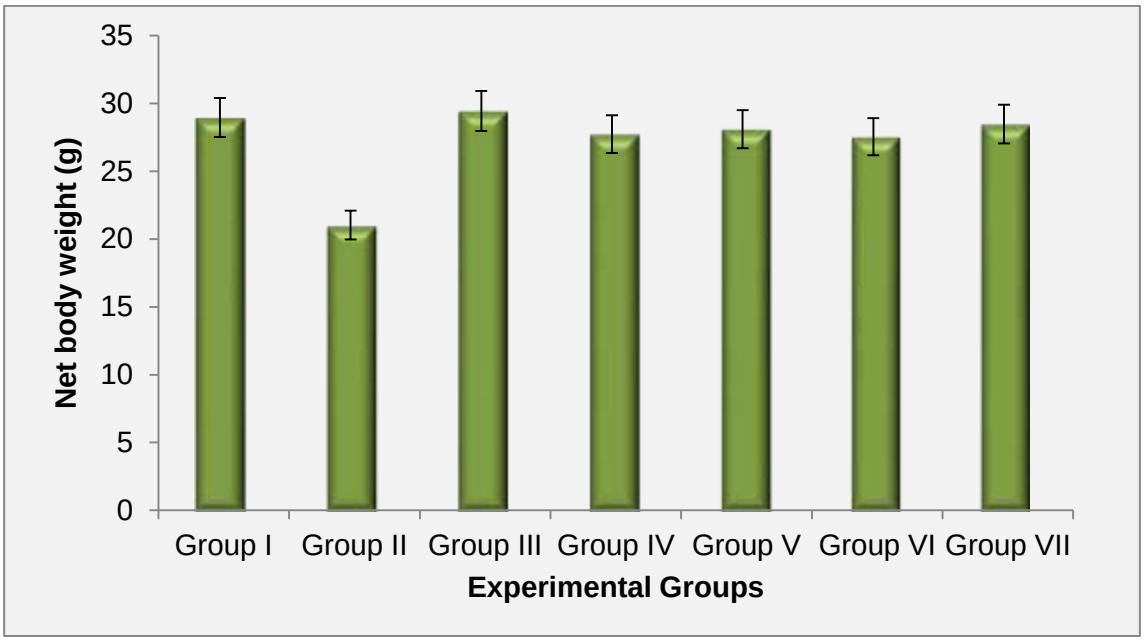


Fig. 41 Body weight of the experimental mice under various treatments

Results in the present study revealed that decrease in body weight of B(a)P treated mice may be due to malabsorption or decreased food intake leading to slaying of skeletal muscle and adipose tissue, cancer, cachexia and anorexia (Rajendran *et al*., 2014). Increase in body weight and decrease in lung weight in the B(a)P treated animals with rhaponticin represented its defensive efficacy, reduces the proliferation, inflammation and tumor growth (Wang *et al*., 2021).

### 4.6.2.4 Analysis of relative lung weight

The effect of relative lung weight on experimental groups (control and treated) were depicted in Fig. 42. B(a)P treated mice revealed significant increase in the lung weight and substantial decrease in the body weight, whereas mice treated with paclitaxel, different doses of syringic acid fraction, syringic acid and

syringic acid alone slowly retained their body weight and drop in lung weight concluded the preclusion of carcinogenesis continuance in B(a)P induced animals.

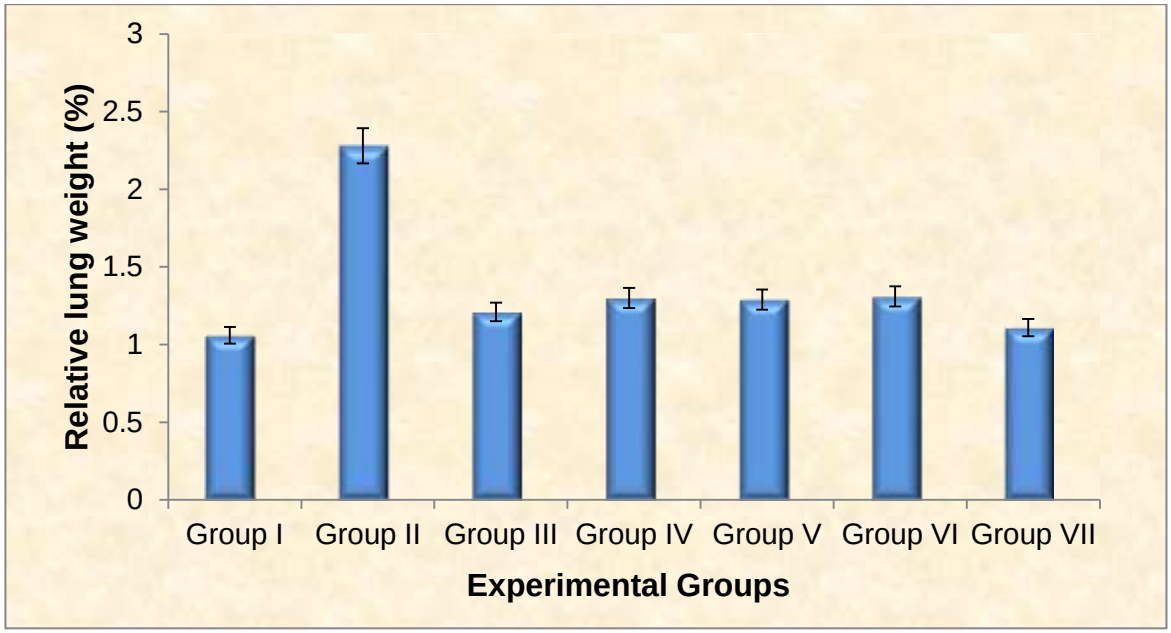


Fig. 42 Relative lung weight of the experimental mice under various treatments

The results of the present study coincides with the findings of Kasala *et al*. (2016) who observed substantial loss in body weight and gain in lung weight against benzo(a)pyrene induced lung carcinogenesis Swiss albino mice. Magesh *et al*. (2006) observed a considerable increase in the relative lung weight due to rapid proliferation of cancerous cell and accumulation of inflammatory cells in lungs. Velli *et al*. (2019) and Wang *et al*. (2014) also reported an increase in body weight and decrease in lung weight in the B(a)P induced mice fed with vanillic acid and rhaponticin. Mice model of NSCLC injected with 6-shogaol (10mg|/kg), a bioactive compound from *Zingiber officinale* significantly reduced the growth and proliferation of lung cancer cells and increased apoptosis (Kim *et al*., 2014). Similarly, allicin (10mg/kg) from *Allium sativum* suppressed the growth of cholangiocarcinoma (Chen *et al*., 2018) and baicalin (50mg/kg) inhibited tumour growth in colon cancer induced mouse by repressing C-Myc and oncomiRs, microRNAs expression to induce apoptosis (Tao *et al*., 2018). Lu *et al*. (2018) administered docetaxel (10mg/kg) and

baicalein (50mg/kg) to NSCLC mice and they noticed decreased tumour growth and angiogenesis by increased apoptosis. Iwanowycz *et al*. (2016) also reported the suppression of $4T_1$ breast tumours in mice administered with emodin which inhibited macrophage filtration and increased the activation of T-cells and reduced tumour angiogenesis.

Thus the increase in body weight and decrease in lung weight of mice administrated with syringic acid fraction represented its protective efficacy against tumour growth as comparable with standard drug paclitaxel and syringic acid.

### 4.6.3. Effect of syringic acid fraction on hematological parameters

Abnormal changes observed in the blood parameters/profile due to the toxic effect of carcinogens or exposure to xenobiotics is an indicator of RBC related diseases. RBCs are often in contact with potentially damaging oxygen levels, but the metabolic activity reverse the injury under normal conditions, which are supported by many defense systems representing their antioxidant activity (Kurata *et al*., 1993).

The values recorded in B(a)P induced mice (Group II) revealed a notable decrease in RBC, haemoglobin and platelets when compared to the control mice (Group I). The B(a)P induced mice administered with syringic acid fraction showed a significant increase ($p<0.05$) in the RBC, haemoglobin and platelet levels as compared with commercial syringic acid and the standard drug, paclitaxel. Similar trend was observed in mice treated with syringic acid alone (Table14).

Table 14. Haematological parameters on B(a)P induced mice under various treatments

| Groups | *Treatment* | RBC ($\times 10^6$ cells/µl) | Hb (g/dl) | Platelets ($\times 10^3$ cells/µl) |
|---|---|---|---|---|
| I | Control | 6.58 ± 0.83 | 11.33 ± 0.40 | 40.1 ± 0.25 |
| II | B(a)P (50 mg/kg) | 3.72± 0.55* | 8.15 ± 0.60* | 36.3 ± 0.19* |
| III | B(a)P + Paclitaxel (5mg/kg) | 5.84 ± 0.79* | 10.86 ± 0.78* | 37.6 ± 0.38* |
| IV | B(a)P + Syringic acid fraction (25 mg/kg) | 5.21 ± 0.55* | 9.92± 0.72* | 35.2 ± 0.33* |
| V | B(a)P + Syringic acid fraction (50 mg/kg) | 5.59± 0.55* | 10.18 ± 0.40* | 36.8 ± 0.62* |
| VI | B(a)P + Syringic acid (25mg/kg) | 5.76± 0.61* | 10.64 ± 0.50* | 37.4 ± 0.60* |
| VII | Syringic acid (25mg/kg) | 6.33± 0.33* | 11.16 ± 0.24* | 39.8 ± 0.92* |
| *SEd* | | 0.1591 | 0.1745 | 0.2766 |
| *P<0.05* | | 0.3467 | 0.3803 | 0.6026 |

Values are mean ± SD of triplicates

* - Significant at 5% level - All groups are compared with tumour control

Table 15 WBC and differential leukocyte counts on B(a)P induced mice under various treatments

| Groups | Treatment | WBC (×$10^3$ cells/µl) | Neutrophils (%) | Monocytes (%) | Lymphocytes (%) | Basophils (%) |
|---|---|---|---|---|---|---|
| I | Control | 5.37 ± 0.91 | 27.21 ± 0.78 | 0.65 ± 0.15 | 70.81 ± 1.89 | 1.97 ± 0.38 |
| II | B(a)P (50 mg/kg) | 12.42 ± 0.78* | 46.78 ± 0.98* | 0.23 ± 0.07* | 44.24 ± 1.68* | 1.48 ± 0.49* |
| III | B(a)P + Paclitaxel (5mg/kg) | 11.01 ± 0.69* | 44.33 ± 0.83* | 1.98 ± 0.48* | 64.69 ± 1.38* | 3.41 ± 0.54* |
| IV | B(a)P + Syringic acid fraction (25 mg/kg) | 10.42 ± 0.84* | 43.61 ± 0.88* | 1.22 ± 0.35* | 63.75 ± 1.42* | 2.43 ± 0.27* |
| V | B(a)P + Syringic acid fraction (50 mg/kg) | 10.62 ± .641* | 43.89 ± 0.54* | 1.35 ± 0.27* | 63.96 ± 1.26* | 2.88 ± 0.93* |
| VI | B(a)P + Syringic acid (25mg/kg) | 10.83 ± 0.75* | 44.02 ± 0.64* | 1.76 ± 0.39* | 64.08 ± 1.91* | 3.23 ± 0.87* |
| VII | Syringic acid (25mg/kg) | 6.73 ± 0.66* | 27.94 ± 0.49* | 0.72 ± 0.09* | 69.52 ± 1.58* | 2.43 ± 0.76* |
| SEd<br>p<0.05 | | 0.2182<br>0.4755 | 0.0810<br>0.1765 | 0.1488<br>0.3241 | 0.1293<br>0.2818 | 0.1293<br>0.2818 |

Values are mean ± SD of triplicates

* - Significant at 5% level - All groups are compared with tumour control

Results revealed that the lung cancer induced mice exhibited reduction in haemoglobin and RBC levels, which is an indication of anemia. This may be due to the liberation of free radicals from liver injured during B(a)P metabolism, where a proportion might have entered into the blood from liver and affected the membranes of red blood cells. Hence the reduced level of RBC in Group II animals of the present study could be attributed to the disturbed haematopoiesis, reduction in RBC formation or enhanced removal from circulation (Kuhn, 2017). Reduction in Hb and RBC level in B(a)P treated mice may be attributed to the destruction of blood forming organs, cell division and injury in alimentary tract, depletion of components required for the erythroblast differentiation and reticulocyte release from bone marrow and cell loss from circulation by leakage or hemorrhage through capillary wall or by the destruction of mature circulating cells directly (Anandkumar *et al*., 2009). Another, therapeutical problem encountered in Group II animals is hypoxia which results in cellular changes that brings on lethal tumour phenotype. This is remarked by high potency for local invasiveness, spreading of tumour and accelerated malignant progression (Hockel and Vanupel, 2001).

The animals that received syringic acid fraction after B(a)P induction restores the haemoglobin content and RBC level as compared with syringic acid and paclitaxel suggesting the protection of tissue from hypoxia and reduced level of a tumorigenesis. Also they stimulate the formation or secretion of erythropoietin and thereby induces stem cells in bone marrow to synthesis red blood cells. Platelets play a key role in body's innate immune system apart from preventing bleeding in damaged blood vessels, which is supported by tool like receptors on its surface (Cox *et al*., 2011).

In the present study, the level of WBC and neutrophils in tumour bearing mice was doubled 12.42 and 46.78 as compared with the control mice (5.37 and 27.21). The mice administered with syringic acid fractions lowered their levels. The level of lymphocytes, monocytes and basophils were decreased in B(a)P induced mice whereas those administered with and SAF reversed or altered their levels as comparable with paclitaxel and syringic acid (Table 15).

White blood cells, the active units of body's defense system play a vital role in the systemic inflammatory response and provide rapid and powerful immunity against infectious agents present in the body. High WBC count and alterations in differential counts such as neutrophils, monocytes, lymphocytes and basophils have been considered as the hallmark of carcinogenesis, and also an indication of allergies, inflammation or infections in the body. The decrease in WBC and neutrophil levels in the treated groups may be due to the production of granulocytes macrophage colony stimulating factor, regulation of committed stem cells by interleukins in the proliferation, differentiation and maturation of WBC production (Guyton, 2000 and Gananog, 2001), whereas their increase may be due to myeloid leukemoid reaction which is secondary to malignancy (George *et al*., 2012). Lymphocytes play a vital role in immune system and are directed against specific antigens and their number decreases under stressful conditions. Due to the toxic effect of B(a)P they may get migrated to the inflammation site and thereby its level decreases. Basophils play an important role in allergic reaction since it is dispersed in heamatopoietic organs. It also initiates the differentiation which is closely associated with cancer metastasis and its assessment in circulation provides prognostic information in cancer (Sokol *et al*., 2008 and Valastyan and Weinberg, 2011).

The results of the present study coincides with the findings of Nithya *et al.* (2014) who observed a decreased WBC and neutrophil count and increased monocyte, basophils and lymphocytes count in mice administered with thymoquinone. Similarly Asiimwe *et al*. (2014) isolated apigenin from *Plectranthus* which acted as an immunostimulant and anticancer agent in rats induced with BCG. The neutrophil and platelet count increased in ascites tumor bearing mice whereas there was a noticeable reduction in lymphocyte level. The animals fed with 5-fluro uracil and cleistanthin B reversed the above mentioned counts (Thummar *et al*., 2015).

Thus a significant difference was observed in the haematological parameters of B(a)P induced mice treated with different doses of SAF.

### 4.6.4. Effect of syringic acid fraction on liver marker enzymes

The serum of the experimental mice were analysed for the liver marker enzymes such as AST, ALT and ALP and the results were tabulated in Table 16. The activities of AST, ALT and ALP in the serum were significantly ($P<0.05$) increased in B(a)P induced groups as compared to those of control mice. Administration of syringic acid fractions to B(a)P induced mice revealed a significant decrease in AST, ALT and ALP levels when compared with Group III and VI animals. Mice treated with syringic acid alone restored the levels of AST, ALT and ALP as that of normal mice.

Liver, the major organ plays a pivotal role in regulating physiological process such as metabolism, storage, secretion and detoxification in the body. The consumption of free amino acids for building the proteins of rapidly dividing tumour cells may end in the alteration of enzyme activity in liver (Siena *et al*., 2003). When there is damage in hepatic cell membrane, the cytosol enzymes namely aspartate amino transaminase (AST), alanine amino transferase (ALT) and serum alkaline phosphatase (ALP) which are the most sensitive markers employed in the diagnosis of hepatotoxicity are released into the blood. AST and ALT, the intracellular enzymes of blood determines the cellular damage (Oh and Hustead, 2011 and Sallie *et al*., 1997). ALP is a ubiquitous enzyme found in liver, kidney, bone, intestine and placenta, where its role differs. Liver and bone dysfunction and impairment in bile flow or lesions of various types elevate the level of ALP (McPhearson and Pincus, 2017). The increase in the liver marker enzymes in B(a)P treated mice may be due to cellular leakage and loss of functional integrity in liver cell membrane, tissue damage or tumour growth progression (El-Beshbishy, 2005) or metabolic changes in the liver such as hepatitis, cirrhosis and liver cancer (Chalasani *et al*., 2004). Treatment of B(a)P induced mice with syringic acid fractions reverted the levels of serum liver marker enzymes to normal as comparable with syringic acid and paclitaxel.

Table 16. Liver marker enzymes on B(a)P induced mice under various treatments

| Groups | Treatment | ALT (U/C) | AST (U/C) | ALT (U/C) |
|---|---|---|---|---|
| I | Control | 33.12± 0.89 | 28.39 ± 0.82 | 75.32 ± 0.94 |
| II | B(a)P (50 mg/kg) | 43.28± 0.95* | 36.18 ± 0.66* | 88.45 ± 0.86* |
| III | B(a)P + Paclitaxel (5mg/kg) | 37.11± 0.68* | 33.74 ± 0.66* | 82.63 ± 0.72* |
| IV | B(a)P + Syringic acid fraction (25 mg/kg) | 39.06± 0.74* | 35.06 ± 0.79* | 85.01 ± 0.68* |
| V | B(a)P + Syringic acid fraction (50 mg/kg) | 38.35± 0.48* | 34.45 ± 0.51* | 84.74 ± 0.56* |
| VI | B(a)P + Syringic acid (25mg/kg) | 37.63± 0.56* | 33.97 ± 0.62* | 83.24 ± 0.81* |
| VII | Syringic acid (25mg/kg) | 33.72± 0.51* | 29.17 ± 0.84* | 76.03 ± 0.79* |
| | SEd | 0.2062 | 0.2055 | 0.1504 |
| | P<0.05 | 0.4492 | 0.4478 | 0.3277 |

Values are mean ± SD of triplicates

* - Significant at 5% level - All groups are compared with tumour control

Taxol derived from endophytic fungus reduced the elevated levels of AST, ALT and ALP and exhibited chemoprotective effect against cancer bearing rats (Vannila *et al*., 2010). Similarly mice intoxicated with alloxan when administered with ethanolic extract of *Senna auriculata*, *Cassia sophera* and *Cassia fistula* significantly regulated or restored the activity of AST, ALP and ALT thereby indicating the improvement in the functional status of liver cells (Shanmugasundaram *et al*., 2011; Mondal *et al*., 2012 and Pradeep *et al*., 2010).

Thus the results suggest that lung cancer induced mice treated with syringic acid fraction signifies or reduces liver damage as comparable with the positive controls (syringic acid and paclitaxel).

### 4.6.5. Effect of syringic acid fraction on renal markers

The key indicators of kidney functions are measured as urea, uric acid and creatinine in order to further monitor the renal toxicity in the experimental mice. The levels of urea, uric acid and creatinine recorded in the experimental animals were tabulated in Table 17. Results revealed that mice administered with B(a)P alone increased the levels of urea, uric acid and creatinine and their elevated levels were however, significantly ($p<0.05$) brought down as comparable with Group III and VI mice. Animals administered with syringic acid alone showed normal activity as compared with control groups.

Table 17 Renal markers on B(a)P induced mice under various treatments

| Groups | Treatments | Urea (g/dl) | Uric acid (mg/dl) | Creatinine (mg/dl) |
|---|---|---|---|---|
| I | Control | 13.23 ± 0.99 | 4.51 ± 0.31 | 0.82 ± 0.12 |
| II | B(a)P (50 mg/kg) | 18.56 ± 0.92* | 8.01 ± 0.48* | 2.39 ± 0.36* |
| III | B(a)P + Paclitaxel (5mg/kg) | 15.34 ± 0.86* | 5.48 ± 0.52* | 1.02 ± 0.29* |
| IV | B(a)P + Syringic acid fraction (25 mg/kg) | 17.04 ± 0.78* | 6.32 ± 0.63* | 1.92 ± 0.31* |
| V | B(a)P + Syringic acid fraction (50 mg/kg) | 16.43 ± 0.81* | 6.18 ± 0.39* | 1.45 ± 0.27* |
| VI | B(a)P + Syringic acid (25mg/kg) | 15.91± 0.72* | 5.93 ± 0.69* | 1.13 ± 0.22* |
| VII | Syringic acid (25mg/kg) | 13.82 ± 0.77* | 4.73 ± 0.73* | 1.03 ± 0.20* |
| | SEd | 0.9413 | 0.0531 | 0.0767 |
| | P<0.05 | 2.0510 | 0.1157 | 0.1672 |

Values are mean ± SD of triplicates

* - Significant at 5% level - All groups are compared with tumour control

Kidney performs elimination of toxic substances produced during metabolism, regulates hemostasis and hormone production which assess the renal state. The rate of excretion of creatinine, a metabolite of creatine phosphate may be lowered than its release from skeletal muscles at the time of kidney damage or failure, thereby the serum levels of creatinine and urea increases accordingly (Khoo *et al.,* 2010). Similarly, uric acid an end product of purine metabolism is also regarded as a marker of oxidative stress also act as an pro-oxidant at elevated levels and its release into circulation increases the level of phosphate and potassium when tumour cells are destructed rapidly (Zahan *et al*., 2011).

The study conducted by Longchar and Prasad (2015) revealed that cisplatin induced Swiss albino mice increased the level of urea and creatinine, which may be due to the decreased glomerular filtration rate or increased ROS, indicating nephrotoxicity. However, treatment with ascorbic acid and cisplatin decreased the level of urea and creatinine signifying the involvement of antioxidant property to scavenge cisplatin-mediated free radical generation. Administration of 400mg/kg of *Citrus reticulata* (Mandarin) peel extract to $K_2Cr_2O_7$ induced male Wistar albino rats exhibited a significant decrease in AST, ALT, creatinine, urea and uric acid levels as compared to $K_2Cr_2O_7$ groups (Bashandy *et al*., 2020).

### 4.6.6 Effect of syringic acid fraction on tumour marker enzymes

The effect of syringic acid fraction on Swiss albino mice in terms of tumour marker enzymes such as gamma glutamyl transferase (GGT), lactate dehydrogenase (LDH) and adenosine deaminase (ADA) are presented in Table 18. It was observed that the serum of tumour bearing mice revealed increased level of GGT, ADA and LDH levels whereas those administered with SAF, syringic acid and PA decrease the level of tumor marker enzymes significantly ($p<0.05$).

Table 18 Tumor markers enzymes on B(a)P induced mice under various treatments

| Group | Treatment | GGT (IU/C) | ADA (µg/ml) | LDH (IU/C) |
|---|---|---|---|---|
| I | Control | 12 ± 0.38 | 113 ± 0.98 | 2247.0 ± 1.8 |
| II | B(a)P (50 mg/kg) | 23 ± 0.42* | 198 ± 0.89* | 3021.0 ± 1.7* |
| III | B(a)P + Paclitaxel (5mg/kg) | 19 ± 0.51* | 115 ± 0.83* | 2652.3 ± 1.1* |
| IV | B(a)P + Syringic acid fraction (25 mg/kg) | 24 ± 0.34* | 129 ± 0.86* | 2301.3 ± 0.9* |
| V | B(a)P + Syringic acid fraction (50 mg/kg) | 22 ± 0.29* | 124 ± 0.93* | 2692 ± 0.41* |
| VI | B(a)P + Syringic acid (25mg/kg) | 21 ± 0.46* | 119 ± 0.96* | 2678 ± 1.36* |
| VII | Syringic acid (25mg/kg) | 14 ± 0.53* | 114 ± 0.81* | 2252 ± 1.24* |
| | SEd | 0.0996 | 0.1020 | 0.0720 |
| | P<0.05 | 0.2169 | 0.2222 | 0.1569 |

Values are mean ± SD of triplicates

* - Significant at 5% level - All groups are compared with tumour control

GGT, a membrane bound enzyme involves in glutathione metabolism cleaves the gamma glutamyl peptide bond and transfers the glutamyl moieties to acceptor molecules. Serum GGT is regarded as a surrogate marker and determinant of non alcoholic fatty liver disease since its leads to oxidative stress and hepatocellular damage (Hossain *et al*., 2016). Corti *et al*. (2009) reported that iron dependent DNA oxidative damage can be enhanced by GGT activity which symbolizes the prospectiveness in the progression of neoplastic transformation. GGT's pro-oxidant activity can contribute to the instability of cancer genome and thereby promotes oxidative DNA damage, implying a role for membrane bound GGT in tumour growth. Treatment of B(a)P induced mice with syringic acid

fractions significantly ($p<0.05$) reversed or reduced the elevator level of GGT to normal, probably by retaining the integrity of hepatocellular membrane, and the reduction rate was comparable with that of standard syringic acid and paclitaxel. Administration of root extract of *Cassia occidentalis* and fruit extract of *Cassia fistula* decreased the GGT level in liver injured experimental mice which were treated with carbon tetrachloride and bromobenzene (Usha *et al*., 2007 and Kalantari *et al*., 2011).

ADA, tumor marker enzymes catalyse the deamination of adenosine to inosine, which can then be deribosylated and transformed to hypoxanthine, an intermediate of purine nucleotide synthesis. The rapidly proliferating cancer cells need hypoxanthine for DNA synthesis (Sauer *et al*., 2012 and Akyol *et al*., 2001). Increased ADA activity in B(a)P treated mice, indicates accelerated salvage pathway, in which more nucleotides are provided to cancer cells that are rapidly multiplying. Treatment with syringic acid fraction significantly ($p<0.05$) decreased the elevation of ADA activity in B(a)P treated mice as comparable with syringic acid, paclitaxel and also the rate of proliferating cancer cells were decreased, thereby highlighting the antiproliferating effect. In line with the present study it has been reported that B(a)P administered Swiss albino mice treated with *Cuphea ignea* extract suppressed the elevation of ADA activity and reduced the level of tumor (Hassan *et al*., 2019).

Similarly, the level of serum LDH, a prognostic biomarker of different types of cancer was elevated in the mice administered with B(a)P. In the regulation of glycolysis, LDH plays a vital role by accelerating energy for the growth of tumour cells (Asokkumar *et al*., 2012 and Anandakumar *et al*., 2009) and also for the proliferation and survival of cancer cells (Xie *et al*., 2014). Thus, increase in LDH activity in cancer induced animals may be due to high rate of proliferating cancer cells. Administration of SAF, to the lung cancer induced mice significantly ($p<0.05$) decreased the rate of proliferating cancer cells as comparable with syringic acid and PA.

The results of the present study are in accordance with the findings of Brihoum *et al*. (2018), where the male albino Wistar rats treated with ethanolic extract of *Propolis* brought down the level of LDH close to control suggesting its beneficial effects. The momentous raise in the LDH level in B(a)P induced mice were reverted back when supplemented with zinc loaded syringic acid thereby signifying its anticancer property (Yang *et al*., 2020).

### 4.6.7. HISTOPATHOLOGICAL STUDIES OF THE LUNG TISSUES

The histopathological investigation of the lung section of control and experimental mice were potrayed in Fig. 43. The control mice (Group I) illustrated normal histological architecture with small uniform nuclei, patent alveoli, and the intervening bronchioles were lined with pseudo - stratified columnar ciliated epithelial cells. The alveoli revealed normal cytological patterns and cell alignment. The interstitium displayed mild multifocal exudates of inflammatory cells with mature lymphocytes. The mice induced with B(a)P (Group II) displayed necrotic lungs with merged pulmonary lobules and the alveoli were damaged as observed from hyperchromatic and irregular nuclei. Also they possessed a well defined tumor with a surrounding intact fibrous capsule which is formed of compact papillae lined by stratified columnar epithelial cells. Diffused marked epithelial cells infolding with minimal dysplasia was observed in Group IV animals. Supplementation of mice with paclitaxel, syringic acid fraction and syringic acid (Group III - VI) abridged the alveolar impairment thereby protecting the neural structures. The mice treated with syringic acid alone (Group VII) did not show any impairment in the histoarchitecture of lung tissues. Wang *et al*. (2021) reported distorted histomorphology of lung tissues in B(a)P induced mice, whereas the animals supplemented with rhaponticin displayed decreased alveolar injury with normal histoarchitecture. Thus the histopathological studies of lung tissue observations suggest that SAF decreases the rate of tumor induction as comparable with PA and syringic acid and ameliorate the biochemical parameters and could be useful for lung cancer therapy.

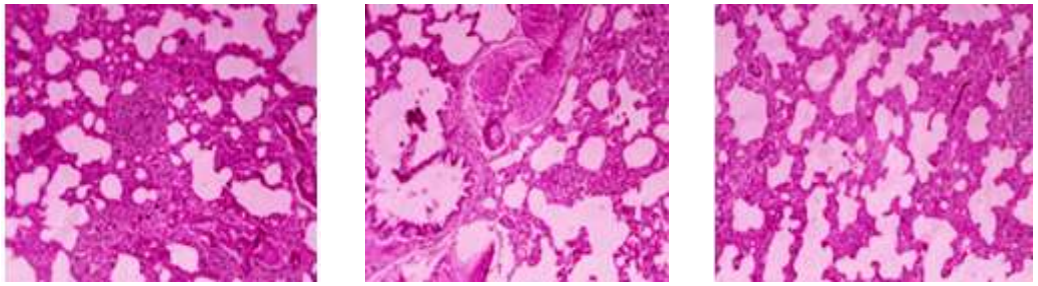

a) Control b) Benzopyrene c) B(a)P + Paclitaxel

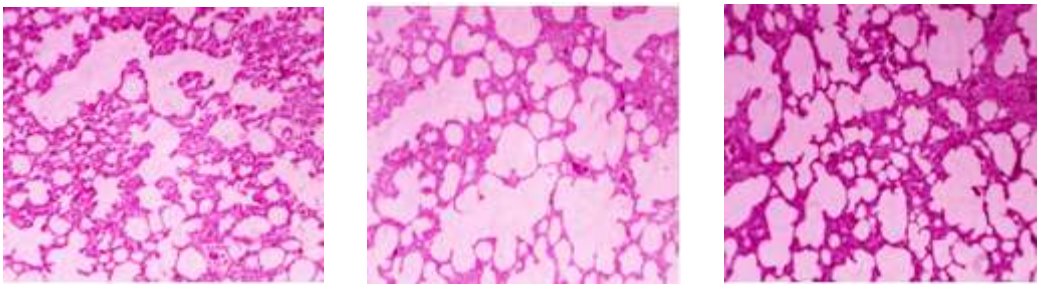

d) B(a)P + SAF (25mg/kg) e) B(a)P + SAF (50mg/kg) f) B(a)P + SA (25mg/kg)

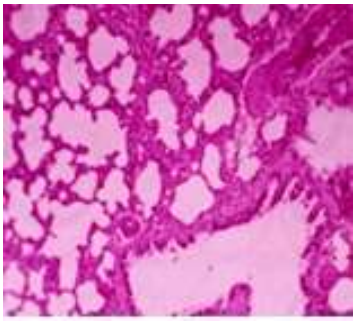

g) SA alone

Fig. 43(a-g) Histopathological analysis of lung tissues

a) Control b) B(a)P (50mg/kg) c) B(a)P+Paclitaxel (5mg/kg) d) B(a)P+SAF (25mg/kg) e)B(a)P+SAF (50mg/kg) f)B(a)P+syringic acid (25mg/kg) g) Syringic acid alone

Hence, the results of the present study confirm that syringic acid fraction plays an incredible defensive role against lung carcinogenesis as comparable with commercial syringic acid and standard drug, paclitaxel and also they have the potential to perform as an efficient phenolic compound against BAP-provoked lung carcinogenesis animal model.